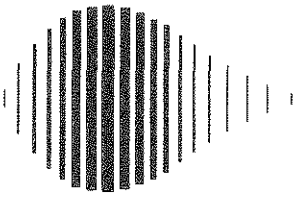

NATIONAL CENTER FOR EARTHQUAKE
ENGINEERING RESEARCH
State University of New York at Buffalo

SEISMIC FRAGILITY ANALYSIS OF SHEAR WALL STRUCTURES

by

Jing-Wen Jaw and Howard H.M. Hwang
Center for Earthquake Research and Information
Memphis State University
Memphis, Tennessee 38152

Technical Report NCEER-88-0009

April 30, 1988

This research was conducted at Memphis State University and was partially supported by the National Science Foundation under Grant No. ECE 86-07591.

NOTICE

This report was prepared by Memphis State University as a result of research sponsored by the National Center for Earthquake Engineering Research (NCEER). Neither NCEER, associates of NCEER, its sponsors, Memphis State University, nor any person acting on their behalf:

a. makes any warranty, express or implied, with respect to the use of any information, apparatus, method, or process disclosed in this report or that such use may not infringe upon privately owned rights; or

b. assumes any liabilities of whatsoever kind with respect to the use of, or for damages resulting from the use of, any information, apparatus, method or process disclosed in this report.

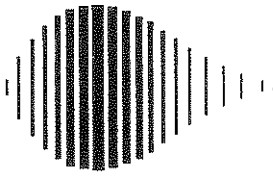

SEISMIC FRAGILITY ANALYSIS OF SHEAR WALL STRUCTURES

by

Jing-Wen Jaw[1] and Howard H.M. Hwang[2]

April 30, 1988

Technical Report NCEER-88-0009

NCEER Contract Number 87-1004

NSF Master Contract Number ECE 86-07591

1 Post-Doctoral Research Associate, Center for Earthquake Research and Information, Memphis State University

2 Associate Research Professor, Center for Earthquake Research and Information, Memphis State University

NATIONAL CENTER FOR EARTHQUAKE ENGINEERING RESEARCH
State University of New York at Buffalo
Red Jacket Quadrangle, Buffalo, NY 14261

PREFACE

The National Center for Earthquake Engineering Research (NCEER) is devoted to the expansion of knowledge about earthquakes, the improvement of earthquake-resistant design, and the implementation of seismic hazard mitigation procedures to minimize loss of lives and property. Initially, the emphasis is on structures and lifelines of the types that would be found in zones of moderate seismicity, such as the eastern and central United States.

NCEER's research is being carried out in an integrated and coordinated manner following a structured program. The current research program comprises four main areas:

- Existing and New Structures
- Secondary and Protective Systems
- Lifeline Systems
- Disaster Research and Planning

This technical report pertains to Program 1, Existing and New Structures, and more specifically to Evaluation Methods and Risk Assessment.

The long term goal of research in Existing and New Structures is to develop methods for rational probabilistic risk assessment for damage or collapse of structures, mainly existing buildings, especially in regions of moderate seismicity. The work will rely on improved definitions of seismicity and site response, experimental and analytical evaluations of systems response, and more accurate assessment of risk factors. This technology will be incorporated in expert systems tools and improved code formats for existing and new structures. Methods of retrofit will also be developed. When this work is completed, it should be possible to characterize and quantify societal impact of seismic risk in various geographical regions and large municipalities. Toward this goal, the program has been divided into five components, as shown in the figure below:

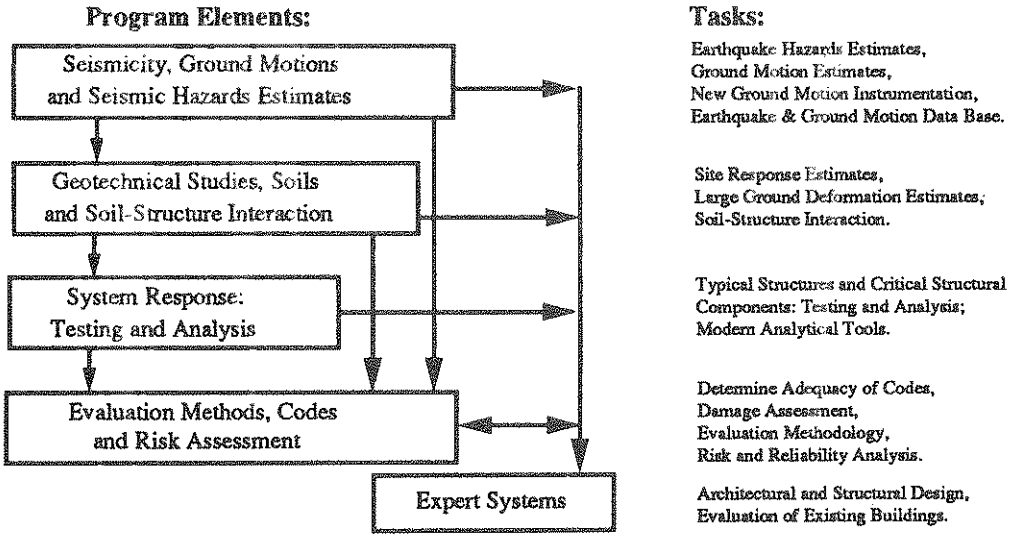

Evaluation Methods and Risk Assessment Studies constitute one of the important areas of research in Existing and New Structures. Current research activities include the following:

1. Development of a damage estimation procedure for the eastern United States.
2. Evaluation of Response Modification Factor (RMF) for buildings and bridges.
3. Development of a probabilistic procedure to determine load and resistance factors.
4. Development of procedures for the evaluation of seismic safety of buildings in zones of moderate seismicity.
5. Development of computer codes for identification of degree of building damage and for damage-based automated design.

The ultimate goal of projects concerned with Evaluation Methods and Risk Assessment is to provide practical tools for engineers to assess seismic risk to individual structures and thus, to estimate social impact.

In this report, analytical procedures for developing fragility curves for building structures are presented and demonstrated with numerical examples carried out on actually designed shear wall structures. As such, this study is useful for urban seismic risk assessment as well as risk assessment of individual building structures.

ABSTRACT

This report presents a fragility analysis method to generate seismic fragility curves for structures, in particular, shear wall structures. Uncertainties including randomness and modeling uncertainty in earthquake ground motion and structure are quantified by evaluating uncertainties in pertinent parameters which define earthquake load-structure system. The uncertainty in each parameter is characterized by several representative values and then the Latin hypercube sampling technique is utilized to combine these values to construct samples of earthquake load-structure system. For the response analysis, the modified Takeda hysteretic model is utilized to describe the nonlinear structural behavior. The nonlinear seismic analyses are performed in time domain for all samples of earthquake load-structure system to obtain an ensemble of structural responses, which are then statistically analyzed. Five limit states representing various degrees of structural damage due to earthquake are established. Then, the statistics of the structural capacity corresponding to each limit state can be established. For a specified level of peak ground acceleration, the limit state probability is evaluated on the basis of statistics of response and capacity for each limit state. The fragility curve is generated by evaluating the limit state probabilities at different levels of peak ground acceleration. For illustration, the fragility curves for a low-rise shear wall building is constructed. The fragility data can be utilized in the seismic risk study to determine potential earthquake-induced loss of life and property damage, then the economic and societal risk can be estimated. In addition, the fragility data can be used by the authority to develop emergency response plan.

TABLE OF CONTENTS

LIST OF ILLUSTRATIONS

LIST OF TABLES

SECTION 1
INTRODUCTION

The occurrence of earthquakes is potentially catastrophic events. A large earthquake may cause loss of lives, damage of buildings, and interruption of essential services (electricity, gas and water, etc.). Thus, the societal and economic impact due to earthquakes and emergency response after earthquakes are the major concerns to governmental agency, e.g., Federal Emergency Management Agency (FEMA), the professional and the general public. In order to determine earthquake-induced loss of life and damage of properties, evaluate economic as well as societal impact, and develop emergency response plan, it is necessary to assess the vulnerabilities of structures due to different levels of earthquakes. Earthquake-induced damage of structures may result from ground failures such as faulting, landslide and liquefaction. The damage of structures, in particular, building structures is mainly due to ground shaking. Thus, earthquake ground shaking is the only hazard source considered in this study.

At a very low level of ground shaking, one can be almost certain that the building would not collapse. Conversely, at an extreme high level of ground shaking, one can reasonably assume that the building would collapse. The likelihood of structural damage due to different levels of earthquakes is usually expressed by a damage probability matrix or a fragility curve [1,2]. The damage probability matrix describes the probability of different possible damages at a specific level of earthquake, while the fragility curve describes the probability of a specific type of damage at various levels of ground shaking. The fragility curve approach is used in this study to express the vulnerabilities of structures.

Fragility data can be generated by using the following: (1) Actual earthquake data; (2) Fragility or qualification test data; (3) Detailed analytical model; (4) Simplified analytical model; and (5) Design information and engineering judgement. The most desirable fragility data are from actual earthquake experience or from experimental tests, since such data (failure or success) provide information with high confidence. When earthquake and test data do not provide sufficient information, simplified or detailed analytical model may be used to predict damage of structures due to earthquakes. The model can include the randomness and uncertainties in earthquake ground motion and structure. The analytical constructed fragility curves should be verified with actual earthquake data, if available.

The use of design information and engineering judgement is the most economical way to construct fragility data. However, the result may be very sensitive to subjective judgment, especially it is based on the opinions of a few engineers [2].

For nuclear structures, several methods have been proposed for generating fragility data for seismic probabilistic risk assessment studies [3-5]. These methods vary from that based on subjective judgement and design drawings to that based on probabilistic structural mechanics. For conventional structures, two recent efforts were made to estimate the vulnerabilities of structures. Applied Technology Council (ATC) has conducted a project to develop earthquake-induced damage data for facilities in California (ATC-13) [1] . The damage data were developed based on the experience and judgement of engineers, who participated in the questionnaire process for consensus damage estimation. Currently, an effort is being made to modify the California-based damage data to represent the damage data for the facilities in the eastern United States. Another effort was made as part of Central United States Earthquake Preparedness Project [6]. As subcontract to Allen and Hoshall, Inc., Kircher and McCann [7] developed seismic fragility curves for sixteen types of structures common to facilities located in the Mississippi Valley region. Fragility curves for structures were mainly produced by calculations blended with engineering judgment. An attempt to calibrate with damage data observed from past earthquakes was also carried out. In performing fragility calculations, the procedure similar to the so-called Zion method [8], which is heavily rely on engineering judgment, was employed for the purpose of rapid curve development.

In view that the earthquake-induced damage data are too scarce to provide sufficient information for the fragility evaluaion, and the fragility data estimated from engineering judgment may not be reliable, therefore, the fragility data generated from analytical models and calibrated with available earthquake experience may be an alternative. Since the detailed analytical model such as the time history analysis with finite element modeling of structures may be too expensive to carry out, the simplified analytical model seems more appropriate for the purpose of fragility evaluation. This report presents a simplified analytical approach to generate fragility data for structures, in particular, shear wall structures. The general methodology is described in Section 2, while Section 3 gives the fragility estimate of a shear wall structure. Then, Section 4 presents the conclusions.

SECTION 2
METHODOLOGY OF FRAGILITY ANALYSIS

The generation of fragility curves for structures by using an analytical approach requires to consider appropriate models for earthquake accelerations and structures. In reality, the earthquake ground accelerations and structures involve randomness and other uncertainties. For example, we cannot predict the occurrence of an earthquake in advance and cannot precisely estimate its amplitude, frequency content and duration. Structural responses are usually evaluated with idealized structural models, thus, the computed structural responses may deviate considerably from the actual structural responses. Furthermore, the structural capacity cannot be accurately determined since the basic parameters such as material strength always exhibit statistical variation. In view of uncertainty in earthquake loads, structural response, and structural capacity, a probabilistic approach, which can incorporate the uncertainty arising from different sources, is appropriate for generating seismic fragility data. In this study, uncertainties including randomness and modeling uncertainty in earthquake ground motion and structure are quantified by evaluating uncertainties in pertinent parameters which define earthquake load-structure system. Figure 2-1 outlines the procedure for the proposed fragility analysis method and the important features are described in the following sub-sections.

2.1 Nonlinear Seismic Analysis

In order to evaluate the statistics of nonlinear structural responses, it is necessary to perform multiple nonlinear time history analyses to obtain the response data. For such purpose, nonlinear seismic analysis with complicated structural modeling such as finite element approach is too expensive to carry out. Thus, a relatively simple structural model which captures the major features of nonlinear characteristics is more appropriate.

In this study, the structure is represented by a multi-degree-of-freedom (MDF) stick model fixed at the base as shown in Fig. 2-2. Each mass is assumed to have one degree of freedom, i.e., the horizontal displacement in the direction of earthquakes. The equations of motion for such an MDF system subjected to a horizontal earthquake ground acceleration is

$$[M]\{\ddot{X}\} + [C]\{\dot{X}\} + \{F_s\} = -[M]\{I\}\ a_g \tag{2.1}$$

where

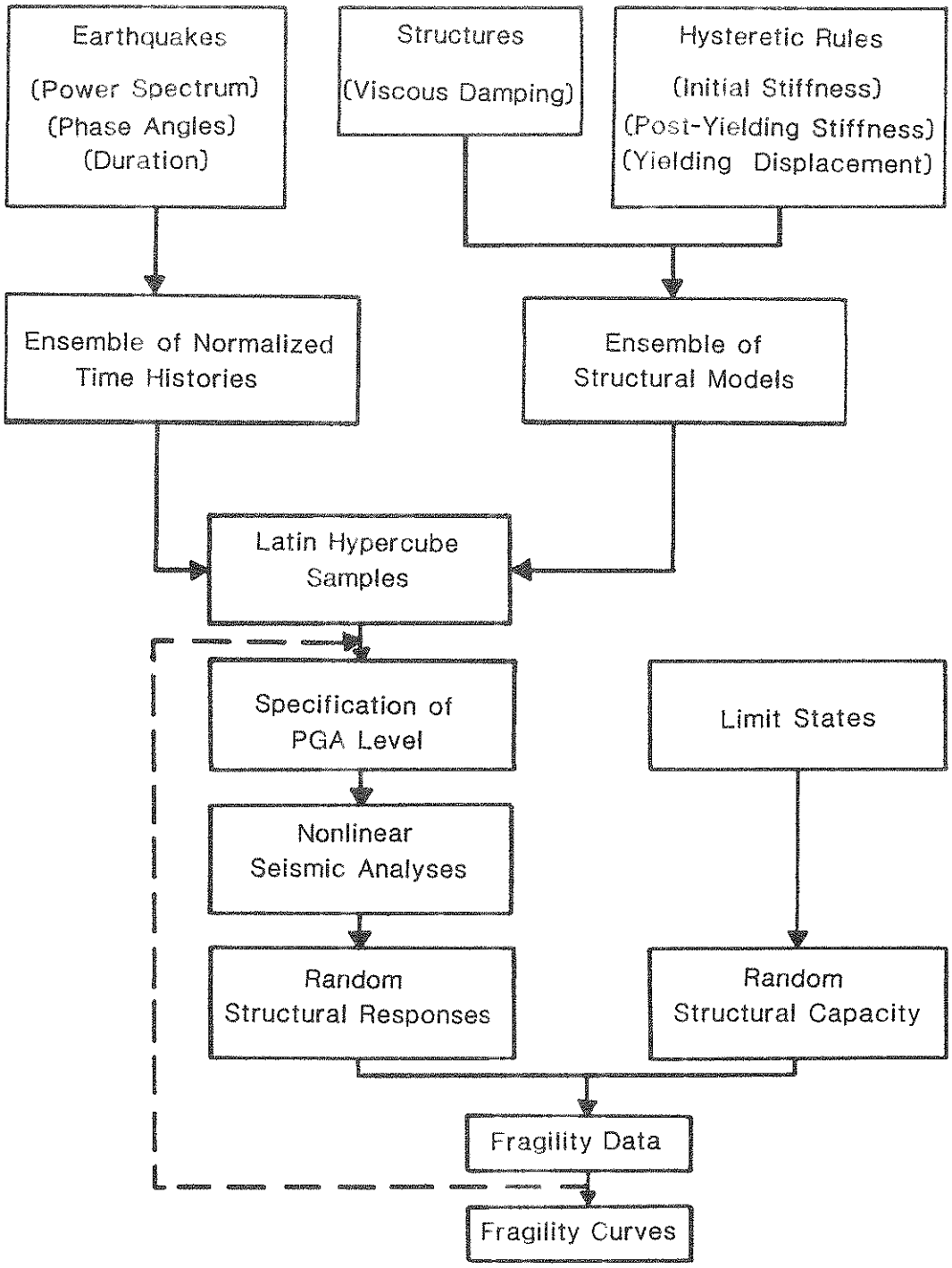

Note: Parameters listed in parentheses are considered as random variables.

Fig. 2-1 Fragility Analysis Procedure

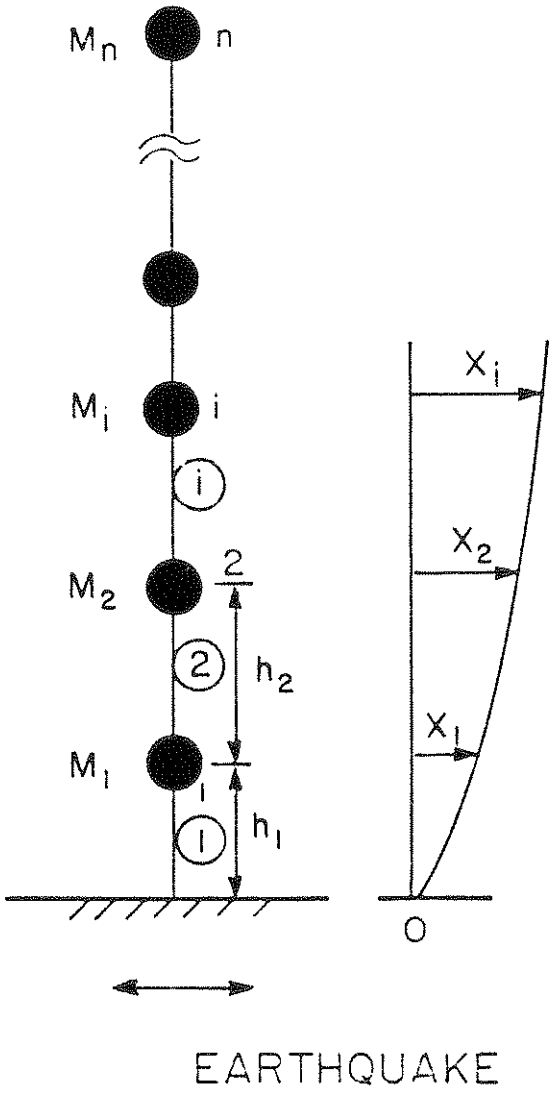

Fig. 2-2 Stick Model of Structure

$[M]$: mass matrix

$[C]$: damping matrix

$\{I\}$: identity vector

$\{X\}$: nodal displacement vector relative to the fixed base

$\{F_s\}$: restoring force vector

a_g: earthquake ground acceleration

The mass of the building is discretized at the mid-height of each story and lumped at the floor level. Thus, the mass matrix $[M]$ is a diagonal matrix. The damping matrix $[C]$ is taken as the Rayleigh damping matrix, which is the combination of the mass matrix $[M]$ and the initial stiffness $[K_e]$ of the structure. The damping matrix $[C]$ is thus given by the equation:

$$[C] = a_0[M] + a_1[K_e] \tag{2.2}$$

where

$$a_0 = \frac{2\zeta\omega_1\omega_2}{\omega_1 + \omega_2}$$

$$a_1 = \frac{2\zeta}{\omega_1 + \omega_2} \tag{2.3}$$

in which ζ is the critical damping ratio; ω_1 and ω_2 are the first two natural frequencies of the structure.

The restoring shear force acting on a beam element of the stick model is related to the relative displacement between two adjacent masses. This displacement is denoted as the inter-node (inter-story) displacement. The structure may behave nonlinearly under severe earthquake excitation. Under this situation, it is generally recognized that the degradation of structural stiffness and pinching phenomenon exist in the hysteretic curves. In this study, the hysteretic relationship between the restoring shear force and the inter-node displacement is modeled by the modified Takeda model [9] as shown in Fig. 2-3. This model has a bilinear skeleton curve and includes both stiffness degrading and pinching effects. The modified Takeda model is governed by the following five rules:

1. Elastic loading and unloading with initial stiffness.
2. Inelastic loading with post-yielding stiffness.
3. Inelastic unloading with degrading stiffness.

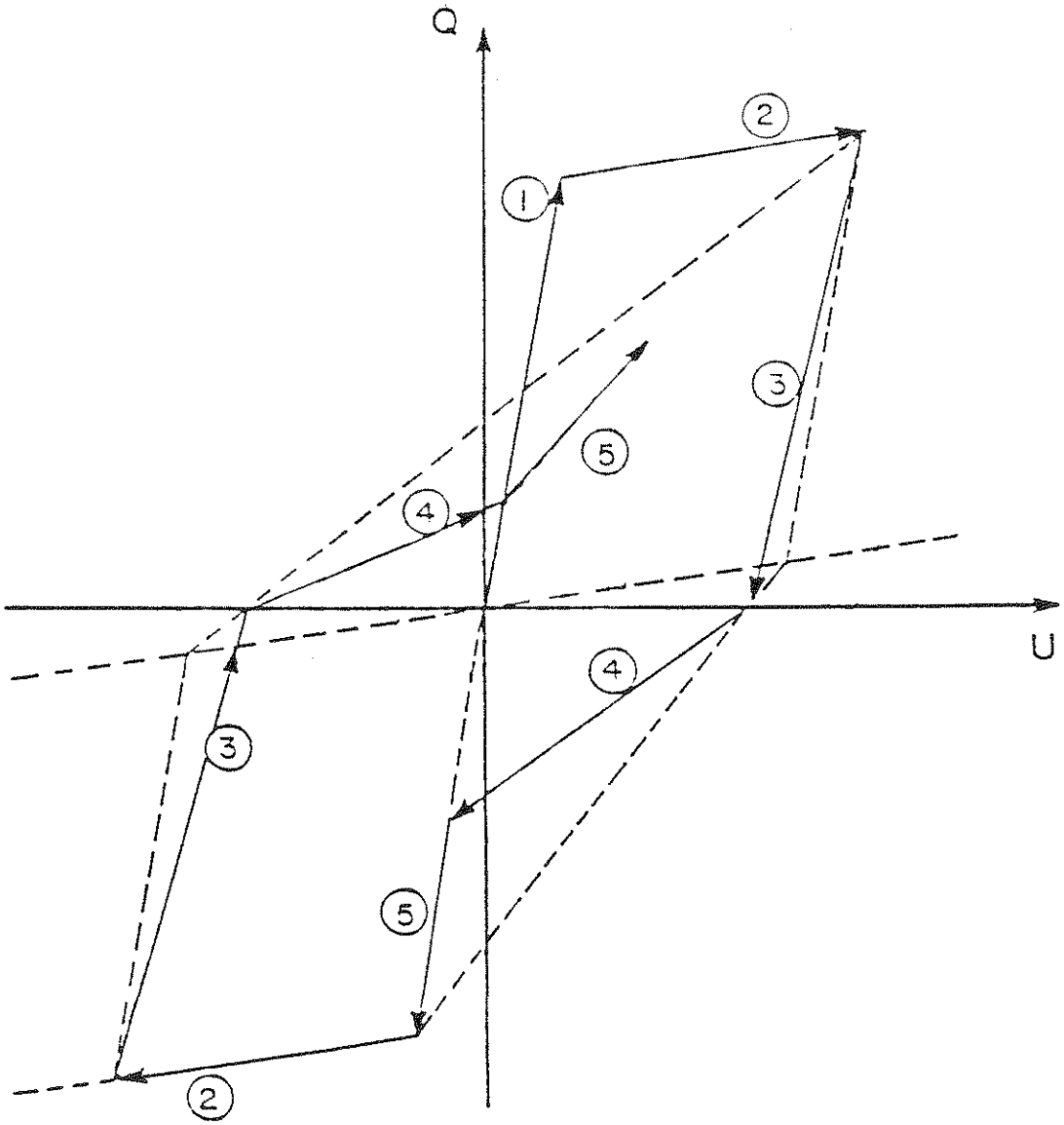

Fig. 2-3 Hysteretic Diagram

4. Inelastic pinched reloading.
5. Peak oriented inelastic reloading.

These five rules result in five possible paths in the hysteretic diagram as identified in Fig. 2-3 by corresponding numbers in circles. Detailed description of the hysteretic rules is presented in Ref. 9. The restoring force vector $\{F_s\}$ in Eq. 2.1 can be derived based on these hysteretic rules.

In this study, the artificial earthquake acceleration time histories are utilized as seismic input and applied at the base of the structure. For a given earthquake time history, the Newmark's beta method with beta equal 1/4 is used to integrate equations of motion in time domain to obtain structural responses.

2.2 Ground Motion Characterization

There are two basic approaches to represent earthquake acceleration time histories. One method is the use of recorded ground motion accelerograms to represent earthquakes that may be expected at a site. Although the number of earthquake records has been increased in past decades, there is a scarcity of strong motion records for some regions, for example, the eastern United States. Aside from the lack of records, neither does this approach grasp the randomness of future earthquakes nor reflect the local site condition. These concerns give rise to the use of simulated artificial earthquake time histories to represent ground motion. Artificial earthquakes may be generated by the following approaches: (1) modify amplitudes and frequencies of actual recorded ground motion accelerograms, (2) develop compatibly from a specified response spectrum, and (3) generate from an appropriate power spectrum. The latter approach, i.e. power spectrum approach, is used in this study.

The stationary acceleration time history $a(t)$ is simulated by the following expression [10].

$$a(t) = \sqrt{2} \sum_{k=1}^{N_f} \sqrt{S_g(\omega_k)\Delta\omega}\ cos(\omega_k t + \phi_k) \tag{2.4}$$

where

$S_g(\omega)$: one-sided earthquake power spectrum
N_f: number of frequency intervals
$\Delta\omega$: ω_u / N_f

ω_u: cutoff frequency

ω_k: $k\Delta\omega$

ϕ_k: random phase angle uniformly distributed between 0 and 2π

The power spectrum used in this study is a Kanai-Tajimi power spectrum [11].

$$S_g(\omega) = S_0 \frac{1 + 4\zeta_g^2 \left(\frac{\omega}{\omega_g}\right)^2}{[1 - \left(\frac{\omega}{\omega_g}\right)^2]^2 + 4\zeta_g^2 \left(\frac{\omega}{\omega_g}\right)^2} \tag{2.5}$$

where S_0 is the intensity of the spectrum which is related to the peak ground acceleration (PGA) [12]; ω_g and ζ_g are the dominant ground frequency and the critical damping, respectively, which depend on the site soil condition.

The normalized nonstationary time history $a_m(t)$ is obtained by applying an envelope function $f(t)$ to a stationary time history $a(t)$, and then normalized by the maximum of the time history a_{max}.

$$a_m(t) = \frac{a(t)f(t)}{a_{max}} \tag{2.6}$$

The nonstationary time history $a_g(t)$ is then obtained from the product of a specified peak ground acceleration A_p and a normalized nonstationary time history $a_m(t)$

$$a_g(t) = A_p \times a_m(t) \tag{2.7}$$

2.3 Uncertainty Analysis

In this study, uncertainties in structure and earthquake ground motion are quantified by investigating the uncertainty in various relevant parameters describing the analytical model for earthquake load-structure system.

2.3.1 Uncertainty in Structural System

The structure is idealized as a stick model with masses lumped at the floor levels. The values of the lumped mass can be determined more or less accurately, thus, the mass is assumed to be deterministic in the present study.

The response of a structure to earthquakes is affected by the energy-dissipation characteristics of the structure. The input seismic energy may be dissipated by structural viscous damping and hysteretic behavior of the structure. It is well known that judgment is usually involved in selecting a value of viscous damping for the dynamic analysis. Therefore, structural viscous damping is treated as random variable and used in conjunction with the structural hysteretic model in the nonlinear seismic analysis.

The modified Takeda hysteretic model utilized in this study is characterized by four parameters: the initial stiffness k_e, the post-yielding stiffness k_p, the yielding displacement U_y, and the pinching factor α_p. These parameters can be determined from the comparison of simulation results and experimental data. However, the values of these parameters determined from the simulation of one experimental work may differ from the values obtained from the simulation of the other experiments. Moreover, even from one simulation, the hysteretic parameters can not be evaluated precisely. For example, it is generally recognized that the initial stiffness k_e is less than the uncracked stiffness due to concrete cracking. The degree of reduction in stiffness can not be determined accurately. Thus, the initial stiffness k_e is treated as random variable. Similarly, the post-yielding stiffness k_p and the yielding displacement U_y can not determine exactly and are also treated as random variables. The pinching of the hysteretic loops is caused by the opening and closing the shear cracks during the cyclic loadings. The degree of pinching in hysteretic loops has a significant effect on the area of hysteretic curve which is related to the amount of energy dissipated under cyclic loading. However, the pinching may have less effect on the maximum deformation of the structure. In this study, the maximum ductility ratio, which is closely related to maximum deformation of the structure, is used to represent the structural response. Thus, it is reasonable to assume the pinching factor as deterministic.

2.3.2 Uncertainty in Ground Motion

The Kanai-Tajimi (K-T) power spectrum is employed in this study to simulate earthquake acceleration time histories. The K-T power spectrum is defined by three parameters S_0, ω_g and ζ_g. The variation of ω_g and ζ_g due to site soil conditions has been examined in several recent studies and the statistics of ω_g and ζ_g for different soil conditions were suggested [13-15]. Thus, in this study, ω_g and ζ_g are considered as random variables. The parameter S_0 in the K-T power spectrum is related to peak ground acceleration. For the purpose of evaluating the fragility of the structure, the peak ground acceleration is

treated as a parameter, hence, S_0 is deterministic. As shown in Eq. 2.4, a set of random phase angles is generated to simulate an acceleration time history. Of course, different sets of random phase angles are utilized to generate a number of acceleration time histories. Furthermore, an envelope function $f(t)$ is applied to a stationary time history so that the earthquake acceleration becomes nonstationary with finite duration. The duration of the strong motion is considered as random in this study.

2.3.3 Analysis of Uncertainty

In this study, the Latin hypercube sampling technique [16] is utilized to establish samples for nonlinear time history analysis. If the simple random sampling technique is used to generate samples, then the required sample size would be very large. Thus, it is not feasible for nonlinear time history response analysis due to the prohibitive cost. On the contrary, the Latin hypercube sampling technique can provide response statistics using a reasonable number of samples [17].

The four parameters describing the structural model, which are treated as random variables, are: structural viscous damping, initial stiffness, post-yielding stiffness, and yielding displacement. The uncertainty in each parameter is characterized by several representative values obtained from available data in the literature. By combination of the representative values of all parameters, a total of N samples of the structural model is constructed. For example, for the four parameters mentioned above, if three representative values are selected to characterize uncertainty in each parameter, then 81 structural models will be created.

To characterize uncertainty in ground motion, two power spectrum parameters, i.e., ω_g and ζ_g, and strong motion duration as well as phase angle are treated as random. The representative values are selected to characterize the uncertainty associated with each parameter. Several power spectra are obtained from combining representative values of ω_g and ζ_g. From each power spectrum, a number of artificial earthquakes are generated by using the selected durations and different sets of random phases angles. The total number of artificial earthquakes should be equal to N which is the same as the number of structural models. Then, following the principle of the Latin hypercube sampling technique, the structural models are matched to the earthquake time histories to construct N samples of earthquake load-structure system for nonlinear seismic analysis.

2.4 Probabilistic Structural Response

For each earthquake load-structure system, nonlinear seismic analysis is carried out to evaluate the responses of the structure, e.g., the story ductility ratios of all stories. The i-th story ductility ratio μ_i is defined as the ratio of the maximum absolute inter-story displacement $U_{max,i}$ to the yielding displacement $U_{y,i}$.

$$\mu_i = U_{max,i}/U_{y,i} \tag{2.8}$$

The maximum ductility ratio of the structure μ_E is the largest value among all story ductility ratios.

$$\mu_E = max(\mu_i) \tag{2.9}$$

In this study, the maximum ductility ratio μ_E is utilized to represent structural response. The N samples of μ_E, which are obtained from time history analyses for all earthquake load-structure systems, is statistically analyzed in order to determine sample mean and sample standard deviation. The data are also plotted in the probability paper to determine the appropriate distribution.

2.5 Limit States and Structural Capacity

In order to generate structural fragility curve, the limit states of a structure must be defined. A limit state generally represents a state of undesirable structural behavior, for example, structural collapse or instability. For a structure, it is likely that more than one limit state has to be considered. The damage of a structure due to earthquakes usually involves nonlinear structural behavior. The presence of the nonlinear behavior makes it difficult to formulate limit states based on strengths of the structure. Various damage models which incorporate maximum deformations and/or energy dissipation have been proposed [18]. However, the use of energy-related damage model to define limit states sometimes is difficult due to the lack of experimental data. In general, both structural and non-structural damages due to earthquakes can be attributed to excessive inter-story displacement. The inter-story displacement is, therefore, a good measure of the degrees of damage. The ductility ratio is closely related to inter-story displacement as indicated in

Eq. 2.8. Thus, in this study, the limit state is defined in terms of the maximum ductility ratio of the structure.

In the event of earthquakes, damage of structures is observed to occur in varying degrees from no damage to collapse. Thus, in this study, five limit states representing nonstructural damage, slight structural damage, moderate structural damage, severe structural damage, and collapse of the structure are considered. For each limit state, a corresponding capacity in terms of the maximum ductility ratio can be established. The structural capacity R is usually modeled by a lognormal distribution [19].

$$R \equiv LN(\tilde{R}, \beta_R) \tag{2.10}$$

where LN stands for the lognormal variable; $\tilde{R}$ and β_R are the median value and the logarithmic standard deviation of R, respectively.

2.6 Fragility Curves

For a given level of peak ground acceleration, the structural fragility with respect to a particular limit state is defined as the conditional probability that the structural response S exceeds the structural capacity R. It can be shown that the conditional limit state probability P_f may be written as [20]:

$$P_f = P_r(R \leq S) = \int_0^\infty [1 - F_S(r)] f_R(r) dr \tag{2.11}$$

where $F_S(\cdot)$ is the cumulative probability distribution of S and $f_R(\cdot)$ is the probability density function of R. The fragility curve for a particular limit state can be constructed by evaluating P_f at different levels of PGA. Fragility curves for various limit states can be developed in a similar manner.

SECTION 3
FIVE-STORY SHEAR WALL BUILDING

3.1 Description of Structure

The building selected to demonstrate the fragility analysis methodology is a five-story reinforced concrete office building assumed to be located in New York City [21]. Figure 3-1 shows a typical floor plan and section of the building. A reinforced concrete frame system is used to resist dead and live loads, while the lateral loads such as earthquakes are resisted by shear walls in both directions. In this study, seismic fragility analysis is performed for the two shear walls in the north-south direction. The detail of the design is shown in Ref. 21, and a brief summary of the design is outlined below.

The shear wall building is designed according to the provisions of ANSI A58.1-1982 Standard [22] and ACI 318-83 code [23]. Three types of loads, i.e., dead, live, and earthquake loads are considered to act on the building. The dead and live loads acting on each shear wall are shown in Ref. 21. Originally, various combinations of seismic zones and soil conditions were considered. In this study, only the design case with seismic zone 2 and soil type 2 is utilized. The design seismic base shear is determined by the formula specified in ANSI A58.1. This design base shear is distributed over the height of the building, and then the shear force and overturning moment at each floor level are determined accordingly. The shear walls are designed to provide sufficient resisting capacity against all postulated combinations of load effects (axial force, shear force, moment, etc.). The cross section and reinforcement arrangement of the shear wall are shown in Fig. 3-2. The barbell shape shear wall is composed of the web wall and two end columns (boundary elements). The thickness of the wall is 5 in. and one layer of No. 3 rebars with 5 in. spacing is used in both horizontal and vertical directions. The end columns are 22 in. $\times$ 22 in. for first and second stories, 20 in. $\times$ 20 in. for third through fifth stories, and 16 No. 9 rebars are used for all end columns.

3.2 Modeling of Structure

The shear wall structure is modeled as an MDF stick model with one degree of freedom per story. The stick model consists of lumped masses connected by beam elements. The convention of numbering nodes and elements is depicted in Fig. 2-2. Table 3-I lists the

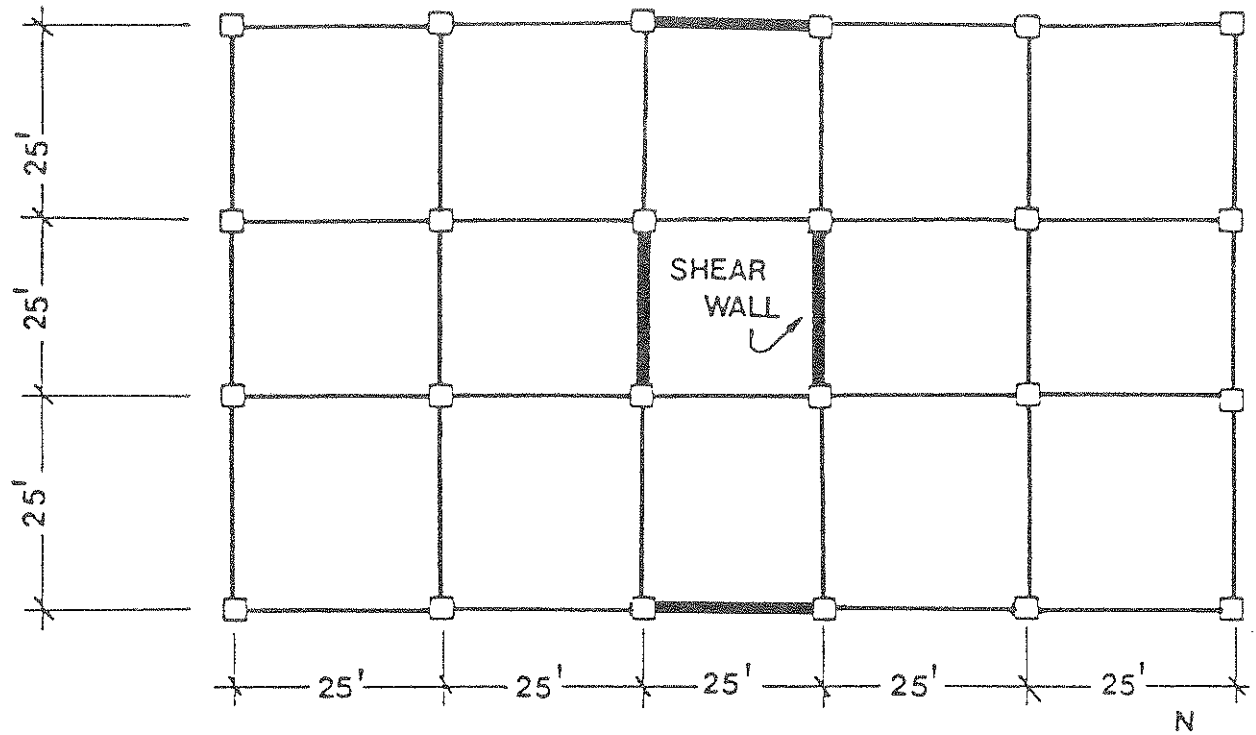

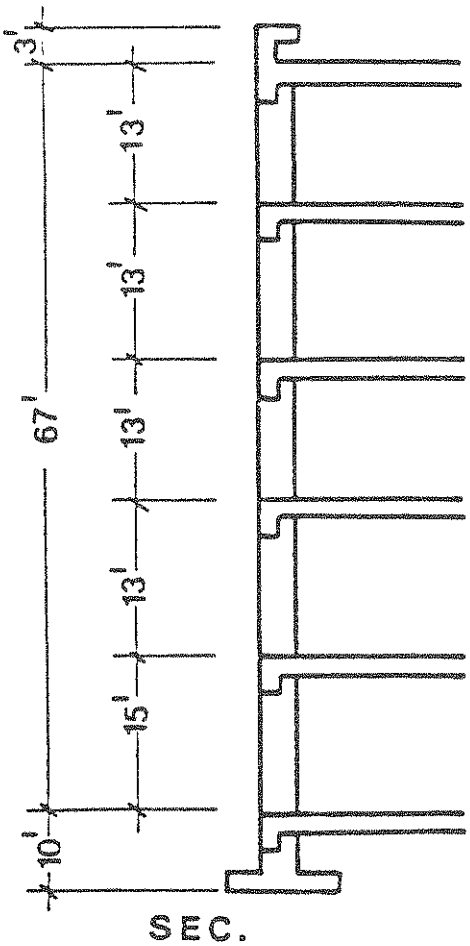

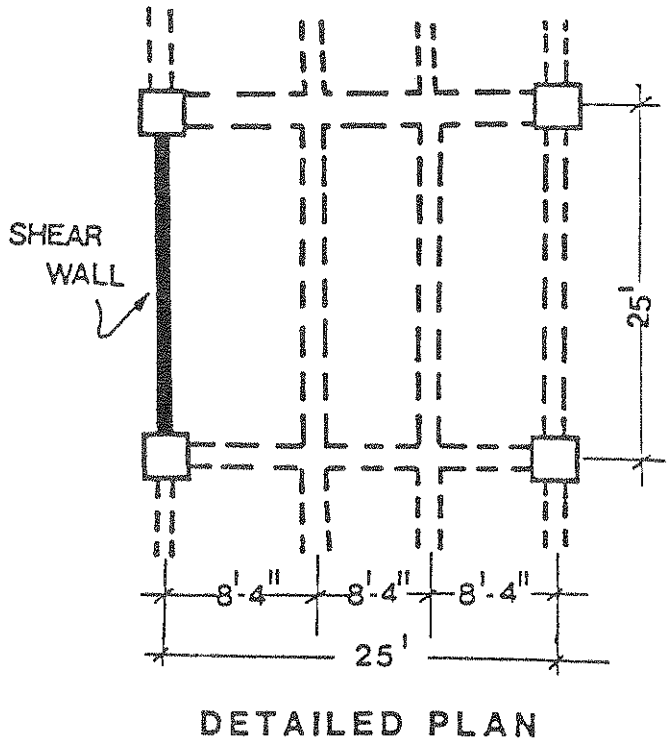

Fig. 3-1 Plan and Section of Office Building

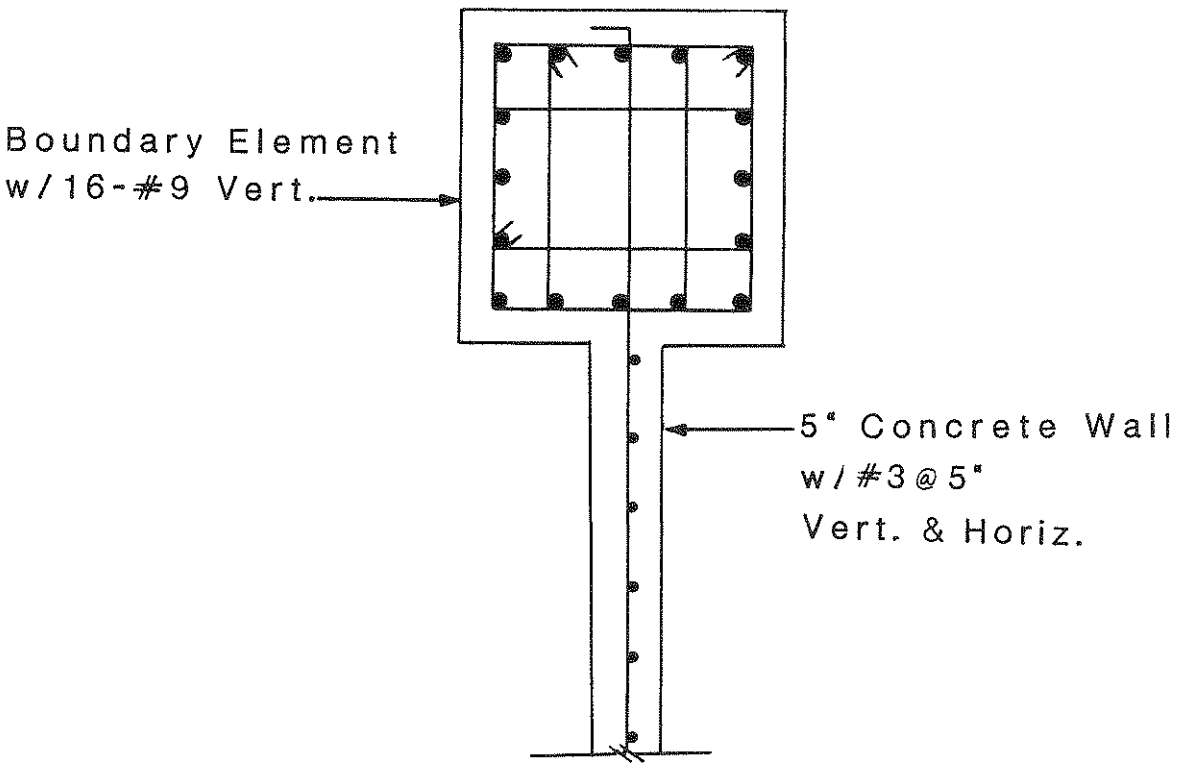

Fig. 3-2 Detail of Shear Wall

Table 3-I Stick Model Properties

Node or Element No.	Mass (kips-sec^2/in)	Element Height (in)	Shear Area (in^2)
5	1.817	156	1400
4	2.105	156	1400
3	2.105	156	1400
2	2.134	156	1390
1	2.199	180	1390

lumped mass at each floor level. The height and effective shear area of beam elements are also included in the table. For shear wall with two boundary columns, the effective shear area is the web area.

The structure dissipates the input seismic energy by structural viscous damping and hysteretic behavior. The structural viscous damping is assumed to represent the energy dissipated within the range of linear elastic response. It has been recommended that the critical damping ratio ranges from 2 to 5 percent for reinforced concrete structures [24]. Thus, three representative values of the critical damping ratio are selected as 2, 4, and 6 percent.

3.3 Hysteretic Model

In this study, the shear force-displacement relationship for each beam element follows the modified Takeda hysteretic model. The parameters defining the hysteretic model are: initial stiffness k_e, post-yielding stiffness k_p, yielding displacement U_y, and pinching factor α_p. These parameters are determined as follows.

Experimental studies of shear walls have indicated that the initial stiffness k_e is significantly less than the uncracked stiffness k_0 due to the existence of the shear cracks. Thus, the initial stiffness k_e can be expressed as the fraction of the uncracked stiffness.

$$k_e = \alpha_g k_0 \tag{3.1}$$

where α_g is the stiffness ratio and the uncracked stiffness k_0 is computed as

$$k_0 = \frac{G_0 A_s}{h} \tag{3.2}$$

in which A_s and h are the shear area and the height of beam element, respectively; G_0 is the shear modulus of the uncracked concrete which is determined from the Young's modulus E_c and the Poisson's ratio ν of concrete.

$$G_0 = \frac{E_c}{2(1+\nu)} \tag{3.3}$$

The stiffness ratio α_g can be deduced from the available experimental results. Bennett et al. [25] summarized the results of both static and dynamic tests for low-rise isolated

and box-like shear walls. The parameter α_g ranging from 0.25 to 0.33 were reported in their investigation. Morgan et al. [26] tested an isolated shear wall under reversing static loads. On the basis of load-deflection diagram from the test as well as concrete cross section and material properties of the wall specimen, α_g is determined to be approximately 0.17. Oesterle et al. [27] conducted an experimental investigation of isolated shear walls subjected to cycling loads. Based on properties of test specimens and envelope curves of measured shear force versus shear distortion, α_g is computed to be 0.16. Tohma and Hwang [28] studied the hysteretic behavior of reinforced concrete containment under cyclic loading. By comparison of the simulated and experimental results, α_g is determined to be 0.07. This relatively low value of α_g is due to the significant shear deformation. Compiling the values of α_g presented above, three values of α_g, namely 0.1, 0.17 and 0.25, are chosen to represent the variation in α_g.

The post-yielding stiffness k_p is expressed as a product of post-yielding slope factor α_s and initial stiffness k_e. The value of α_s is determined empirically by measuring the post-yielding slopes of load-deformation envelopes of two shear wall experiments [26, 27]. α_s is approximately 0.02 for the shear wall considered in Ref. 26 and 0.03 from the test result presented in Ref. 27. It is not uncommon to find the value of α_s ranging from 0 (elasto-plastic system) to five percent is used in many analytical studies. Thus, based on the foregoing data, three values of α_s, i.e., 0.01, 0.03 and 0.05, are chosen to characterize the variation in α_s.

In this study, the yielding displacement U_y of the shear beam is obtained from multiplying the yielding shear strain γ_y by the element height h. The yielding shear strains can be measured from the hysteretic curves. From the hysteretic curves shown in Refs. 26 and 27, three values, i.e. 0.002, 0.0025 and 0.003, are selected as representative values.

The pinching factor α_p needs to be determined so that the hysteretic model could be described completely. The pinching of the hysteretic loops is caused by the opening and closing of the shear cracks during the cyclic loadings. Tohma and Hwang [28] simulated the experimental results to examine the effect of pinching. The pinching factor of 0.3 was suggested to be an appropriate value. The degree of pinching in hysteretic loops has a significant effect on the area of hysteretic curve which is related to the amount of energy dissipated under cyclic loading. However, the pinching may have less effect on the maximum deformation of the structure. In this study, the maximum ductility ratio, which

is closely related to maximum deformation of the structure, is used to represent structural response. Thus, the pinching factor is assumed as deterministic and set to be 0.3.

3.4 Ensemble of Structures

The four parameters describing the model of the structure, which are treated as random variable, are: structural viscous damping, stiffness ratio, post-yielding stiffness, and yielding displacement. The uncertainty in each parameter is represented by 3 values as summarized in Table 3-II. From the combinations of three representative values of these four parameters, a total of 81 structural models can be established.

To illustrate how to construct the structural model from the parameter values taken from Table 3-II, a set of parameters values, e.g. 0.04 for critical damping ratio, 0.17 for stiffness ratio, 0.03 for post-yielding slope factor and 0.002 for yielding shear strain, is utilized. For concrete compressive strength of 3000 psi and the Poisson's ratio of 0.2 as assumed in design [21], the shear modulus of the uncracked concrete G_0 is determined to be 3.1×10^6 psi (Eq. 3.3). Using physical properties of beam elements as shown in Table 3-I, the uncracked stiffness k_0 and initial stiffness k_e of beam elements can be determined from Eqs. 3.2 and 3.1, respectively. Then, the post-yielding stiffness k_p of beam elements are obtained from multiplying initial stiffness by the post-yielding slope factor. From the specified yielding shear strain, the yielding displacement U_y of the element can then be determined from multiplying yielding shear strain by the element height. Once the initial stiffness k_e, the post-yielding stiffness k_p, and the yielding displacement U_y are determined as well as the pinching factor α_p is specified, the hysteretic model for beam elements is established. Table 3-III summarizes the hysteretic model for all the elements of the structure.

The Rayleigh damping is used in this study, which is the combination of the mass and stiffness matrices of the structure, as described by Eq. 2.2. The mass matrix can be constructed from the individual mass values listed in Table 3-I. The stiffness matrix of the structure is formed by assembling the appropriate element initial stiffness given in Table 3-III. From the free vibration analysis of this structural system, the natural frequencies of the first two modes are 8.680 rad/sec and 25.274 rad/sec, respectively. Assuming the critical damping ratio of 4% for these two modes, the coefficients of damping matrix, a_0 and a_1 (Eq. 2.3), are computed as 0.5168 and 0.002356, respectively.

Table 3-II Representative Values of Structural Parameters

Structural Parameter	Representative Values
Critical Damping Ratio ζ	0.02, 0.04, 0.06
Stiffness Ratio α_g	0.10, 0.17, 0.25
Post-yielding Slope Factor α_s	0.01, 0.03, 0.05
Yielding Shear Strain γ_y	0.002, 0.0025, 0.003

Table 3-III Values of Hysteretic Model

Element No.	Uncracked Stiffness k_0 (kips/in)	Initial Stiffness k_e (kips/in)	Post-Yielding Stiffness k_p (kips/in)	Yielding Displacement U_y (in)	Pinching Factor α_p
5	11674	1985	60	0.312	0.3
4	11674	1985	60	0.312	0.3
3	11674	1985	60	0.312	0.3
2	11591	1970	59	0.312	0.3
1	10045	1708	51	0.360	0.3

3.5 Ensemble of Earthquake Time Histories

The earthquake ground motion used in this study is represented by an ensemble of artificial acceleration time histories generated from Kanai-Tajimi (K-T) power spectra. For each power spectrum, two parameters, i.e., ω_g and ζ_g need to be determined. These parameters are dependent on the site soil conditions. The statistics of ω_g and ζ_g for different soil conditions has been reported in several studies [13-15]. Typically, for sites with soft soil condition, ω_g is estimated in the range of 2.4π to 3.5π [14, 15], whereas for rock sites, ω_g is ranging from 8π to 10π [15, 29]. Furthermore, for the stiff soil condition, ω_g is between the values estimated for rock and soft soils. The general soil conditions ranging from soft soil to rock type are reported in the metropolitan area near New York City, where the shear wall structure is assumed to be located. Thus, three values of ω_g, namely, 3π, 6π and 9π are selected as representative values. For the value of ζ_g, it is estimated that the mean value is about 0.6 and coefficient of variation (COV) is about 0.4 [13, 15]. Thus, three values of ζ_g, i.e. 0.6, 0.36 and 0.84 are chosen. These values are corresponding to mean, mean minus and plus one standard deviation of ζ_g. Another parameter in the description of earthquake ground motion is the strong motion duration. Based on the statistics of strong motion duration presented in Refs. 13 and 14, three values of strong motion duration, namely 5, 10, and 15 seconds are chosen as representative values in the present study. The values of ground motion parameters used in this study are listed in Table 3-IV.

From the combinations of three values of ω_g and ζ_g, nine power spectra are obtained. Figure 3-3 shows a power spectrum with ω_g of 6π and ζ_g of 0.36. For each power spectrum, three stationary time histories are generated by utilizing Eq. 2.4. Thus, 27 stationary time histories are produced. It is noted that 27 different sets of random phase angles are used to generate these time histories. An envelope function is applied to a stationary time history to generate a nonstationary ground acceleration (Eq. 2.6). The envelope function used in this study is a trapezoidal shape as illustrated in Fig. 3-4. The rise and decay time of the envelope function are taken as 2.5 seconds. The strong motion duration, which is the time between rise and decay time, is treated as random and three representative values are given in Table 3-IV. By applying the three envelope functions mentioned above to each stationary time history, three normalized nonstationary time histories are generated. Thus, for this study, 81 normalized earthquake acceleration time histories are generated. A sample of generated acceleration time histories is plotted in Fig. 3-5. Using the Latin hypercube

Table 3-IV Representative Values of Ground Motion Parameters

Ground Motion Parameter	Representative Values
ω_g (rad/sec)	3π, 6π, 9π
ζ_g	0.36, 0.60, 0.84
Strong Motion Duration (sec)	5, 10, 15

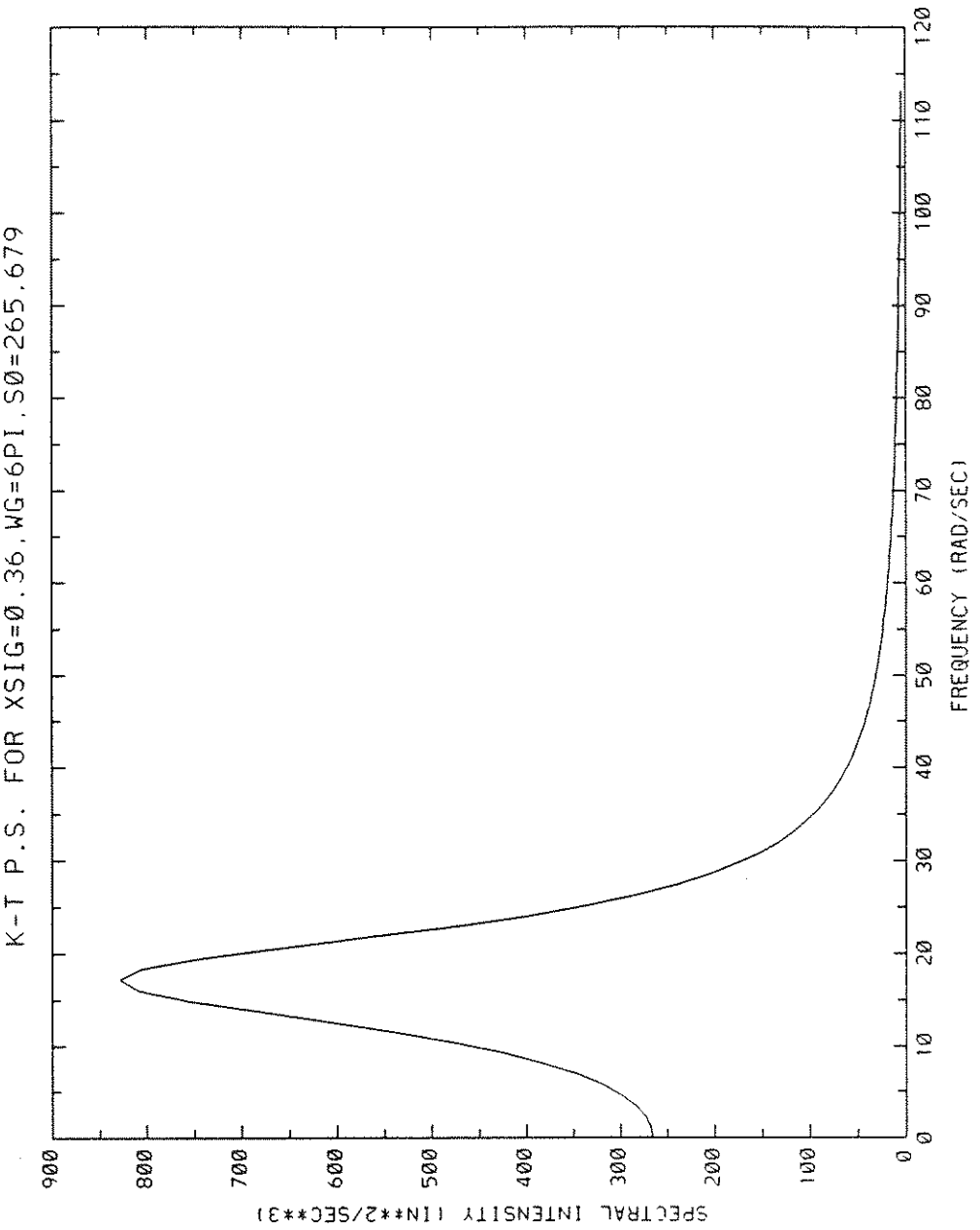

Fig. 3-3 An Example of Power Spectrum

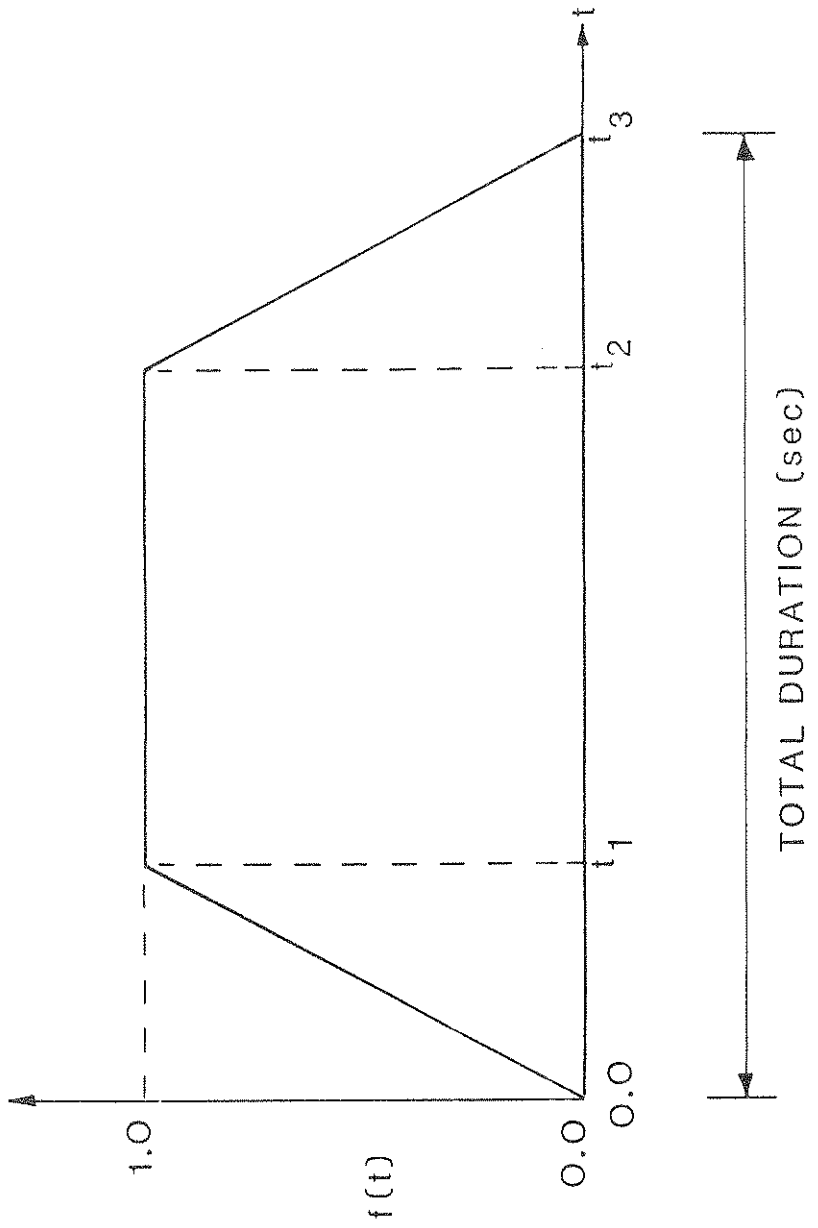

Fig. 3-4 Envelope Function

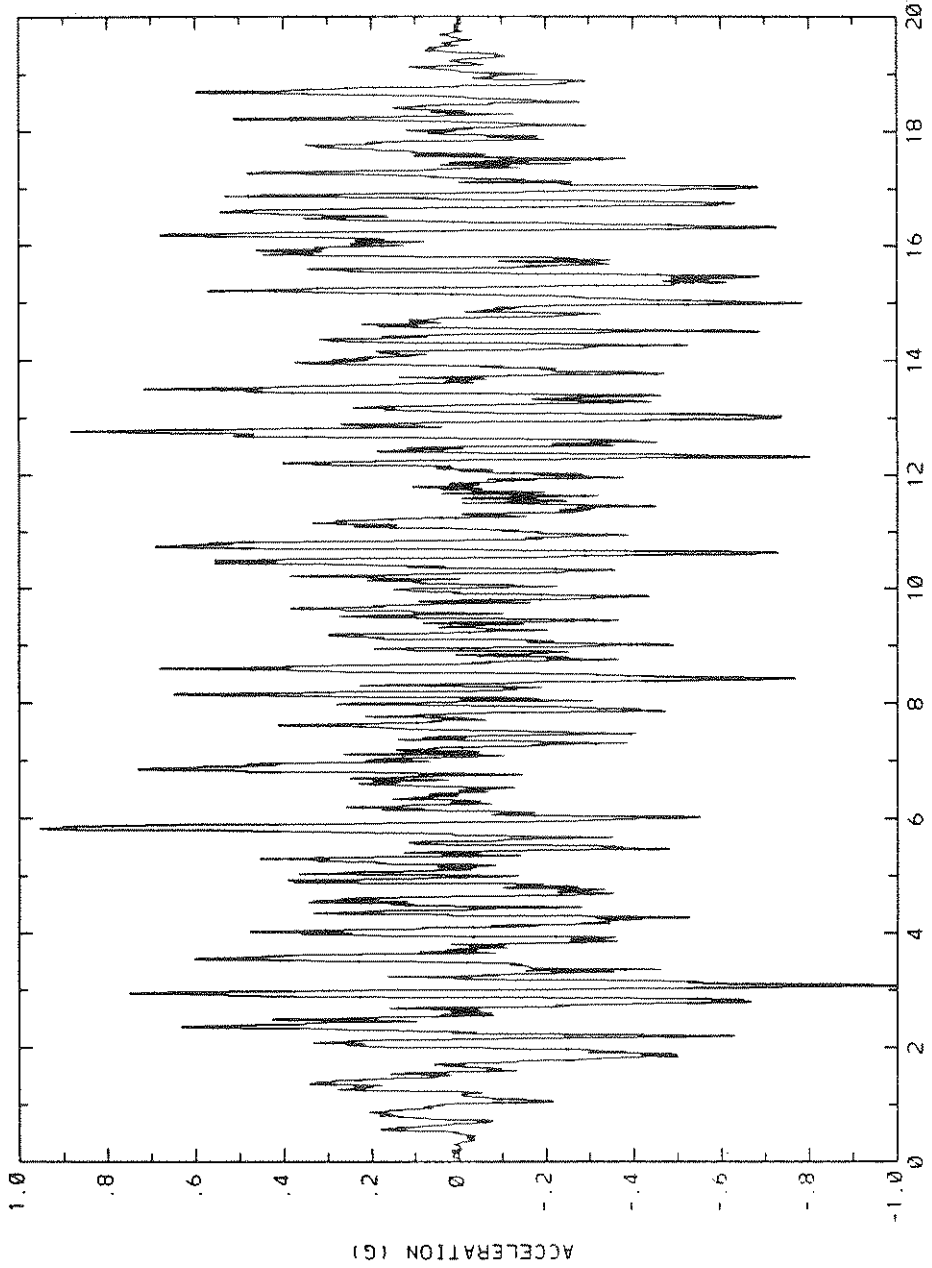

Fig. 3-5 A Sample of Earthquake Time Histories

sampling technique, these earthquake time histories are then matched to the structural models so that 81 samples of the earthquake load-structure system are constructed for seismic response analyses.

3.6 Statistical Analysis of Responses

For a specified PGA level, nonlinear time history analysis is performed for each sample of earthquake load-structure system to evaluate required structural responses. In this study, the maximum ductility ratio is chosen to represent structural responses. Thus, 81 maximum ductility ratios are obtained and then statistically analyzed to evaluate sample mean and sample COV. The 81 samples are also plotted in the probability papers for the lognormal and the extreme Type I distributions. Figures 3-6 and 3-7 show the plots of probability papers with sample data obtained from PGA equal to $0.2g$. From these figures, it can be seen that both distributions fit the data reasonably well. Thus, both lognormal and extreme Type I distributions are utilized to describe the distribution of structural responses. The parameters of the extreme Type I distribution are α and u. For the lognormal distribution, the median $\tilde{\mu}_E$ and logarithmic standard deviation β_E are the parameters of the distribution. The parameters of these two distributions can be determined from the sample mean and the sample COV [20]. For the purpose of constructing fragility curve for the structure, the structural responses corresponding to various levels of PGA need to be evaluated. In this study, 6 levels of PGA ranging from $0.045g$ to $0.6g$ are used. Table 3-V summarizes the statistics of maximum ductility ratios and the parameters of two distributions for all levels of PGA considered.

3.7 Structural Capacity

In the present study, five limit states representing nonstructural damage, slight structural damage, moderate structural damage, severe structural damage, and collapse are established to characterize the degree of damage incurred in buildings during earthquakes. The ductility capacity μ_R associated with a particular limit state is assumed to be lognormal distributed. For the limit state corresponding to collapse of the structure, the median capacity $\tilde{\mu}_R$ and the logarithmic standard deviation β_R are determined from analyzing test data of shear wall specimens [30]. The values of $\tilde{\mu}_R$ and β_R for the other four limit states are assigned based on engineering judgement. Values of $\tilde{\mu}_R$ and β_R for five limit states are given in Table 3-VI.

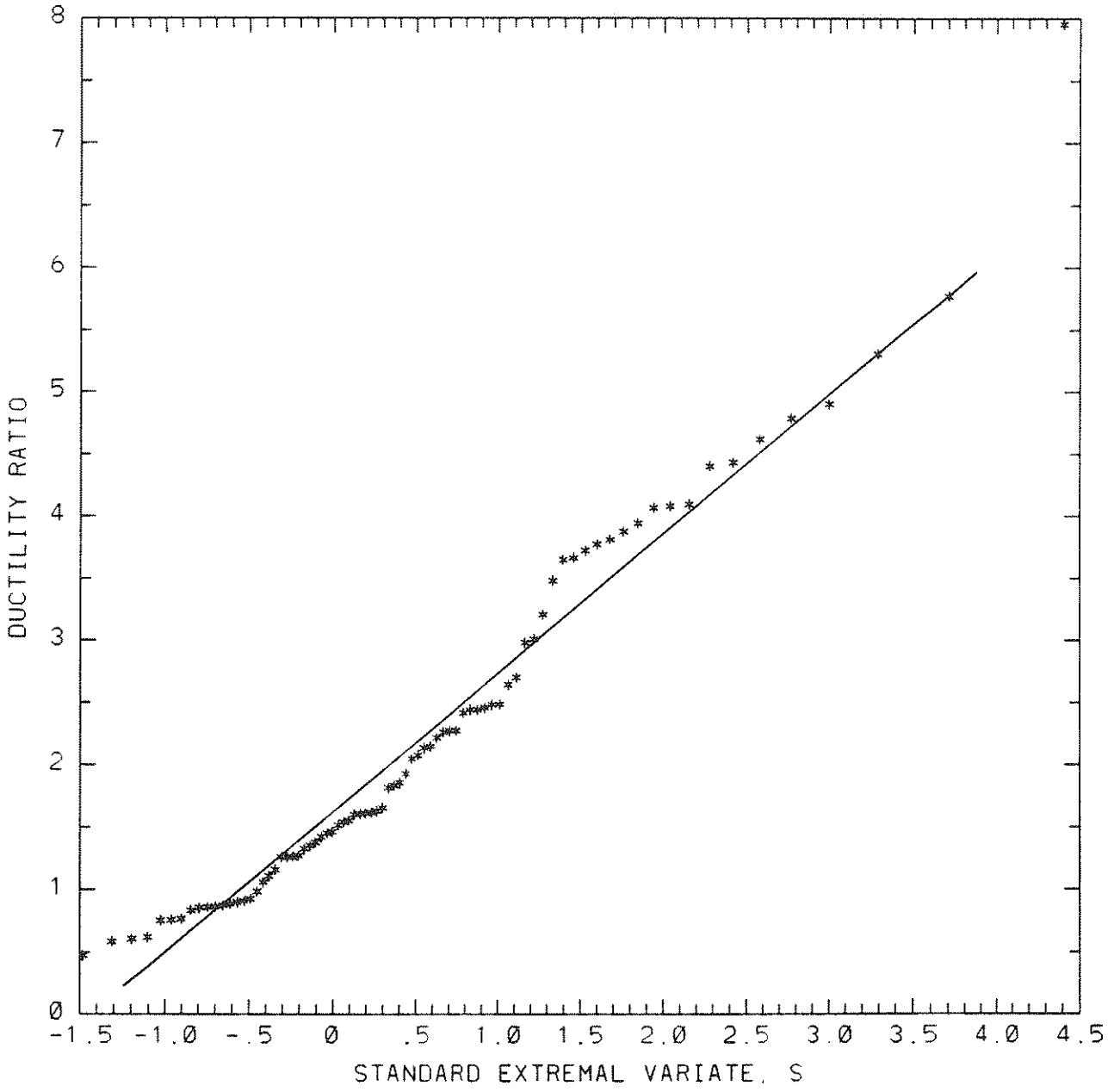

Fig. 3-6 Distribution of Maximum Ductility Ratios (Extreme Type I)

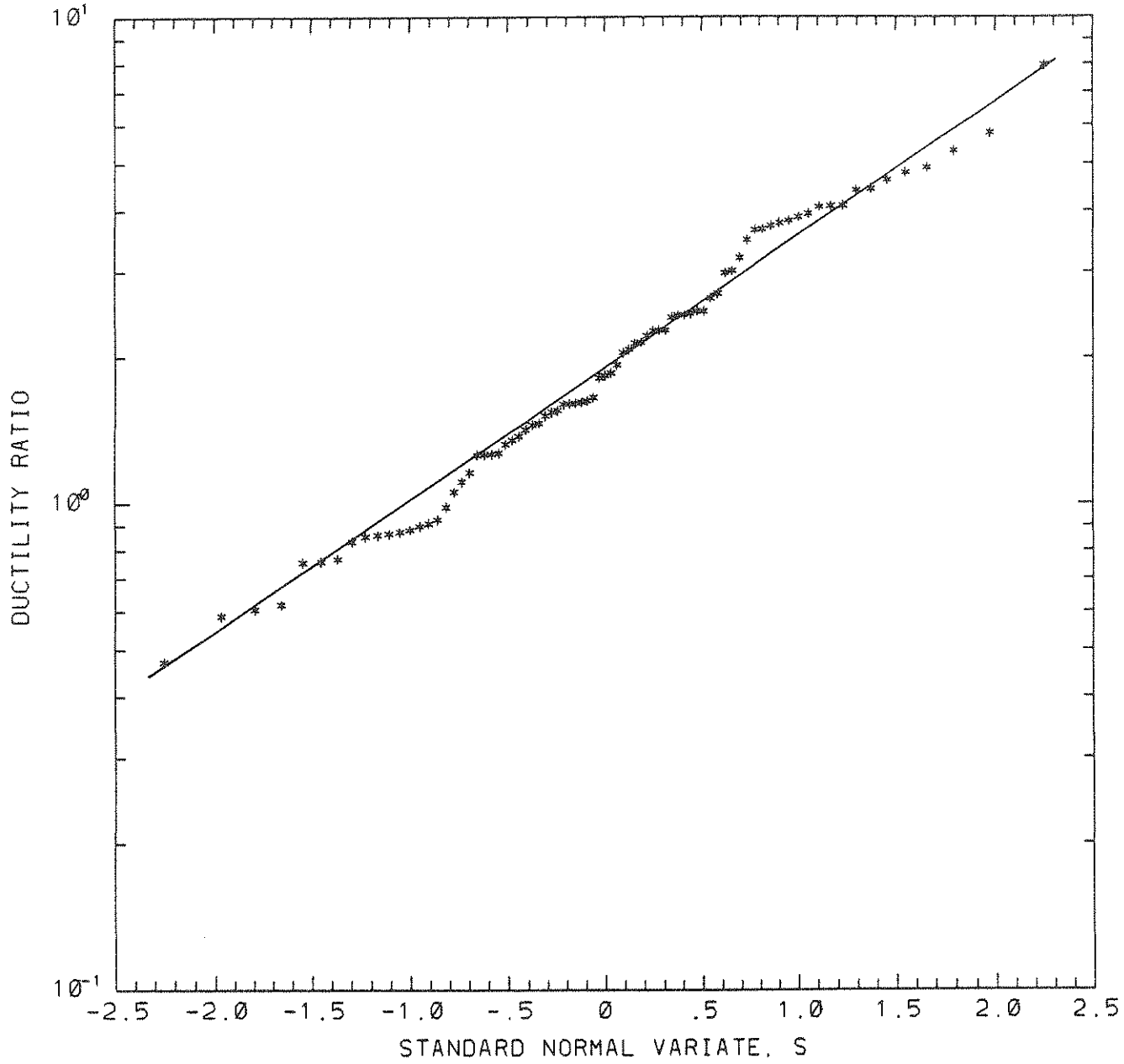

Fig. 3-7 Distribution of Maximum Ductility Ratios (Lognormal)

Table 3-V Statistics of Maximum Ductility Ratios

PGA (g)	Mean	COV	Extreme Type I		Lognormal	
			α	u	$\tilde{\mu}_E$	β_E
0.045	0.408	0.51	6.154	0.314	0.363	0.48
0.075	0.701	0.56	3.250	0.524	0.611	0.52
0.1	0.983	0.63	2.084	0.706	0.833	0.58
0.2	2.259	0.64	0.889	1.609	1.903	0.58
0.4	6.688	0.76	0.253	4.409	5.332	0.67
0.6	12.374	0.69	0.150	8.525	10.179	0.62

Table 3-VI Ductility Capacity

Limit State	$\tilde{\mu}_R$	β_R
Nonstructural Damage	1.0	0.3
Slight Structural Damage	2.0	0.3
Moderate Structural Damage	4.0	0.3
Severe Structural Damage	6.0	0.3
Collapse	7.5	0.3

3.8 Fragility Evaluation

The fragility curve for the structure is the limit state probabilities with respect to a particular limit state at various levels of PGA. The limit state probability for a particular limit state and a specified level of PGA is evaluated from Eq. 2.11. This procedure is carried out for all five limit states and different levels of PGA. For the case (Case I) that the structural responses are described by the extreme Type I distribution, the fragility data are tabulated in Table 3-VII, and fragility curves are plotted in Figs. 3-8 and 3-9. As shown in Fig. 3-8, the fragility data are plotted on semi-logarithmic scale so that the lower tails of the fragility curves can be displayed. Conventionally, the fragility data are displayed on a arithmetic plot as shown in Fig. 3-9 in which the fragility data at higher accelerations are clearly depicted. For the case (Case II) that the structural responses are described by the lognormal distribution, the fragility data are shown in Table 3-VIII and plotted in Fig 3-10. On the basis of these fragility data, several observations are discussed as follows:

(1) For a specified limit state under consideration, the limit state probability generally increases as the PGA value increases. From Table 3-VII, for example, the probability that the shear wall structure may incur moderate structural damage is about 2.50×10^{-6} for PGA of $0.045g$, while it reaches 5.63×10^{-3} for PGA of $0.1g$.

(2) At a particular PGA level, the probability that the structure will damage decreases with the increasing severity of damage level. For instance, at the peak ground acceleration of $0.1g$, the probability of the shear wall building incurring different degrees of damage is in the range of 0.42 (nonstructural damage) to 9.31×10^{-5} (collapse). Thus, the fragility data, such as those shown in Table 3-VII, depict the likelihood that shear wall structures will sustain various degrees of damage at each level of ground shaking induced by earthquakes.

(3) From the fragility data shown in Tables 3-VII and 3-VIII, it is observed that the structure suffers minor damage under small earthquakes and severe damage under larger earthquakes.

(4) The extreme Type I and lognormal distributions are utilized to described the structural responses. The fragility data obtained from the use of these two distributions

Table 3-VII Fragility Data (Case I)

Limit State	Peak Ground Acceleration (g)					
	0.045	0.075	0.1	0.2	0.4	0.6
Nonstructural Damage	3.65 E-2	0.22	0.42	0.80	0.90	0.95
Slight Structural Damage	8.51 E-4	2.32 E-2	9.53 E-2	0.50	0.83	0.93
Moderate Structural Damage	2.50 E-6	4.63 E-4	5.63 E-3	0.14	0.65	0.85
Severe Structural Damage	2.61 E-8	1.83 E-5	4.83 E-4	4.00 E-2	0.48	0.75
Collapse	1.40 E-9	2.19 E-6	9.31 E-5	1.60 E-2	0.37	0.67

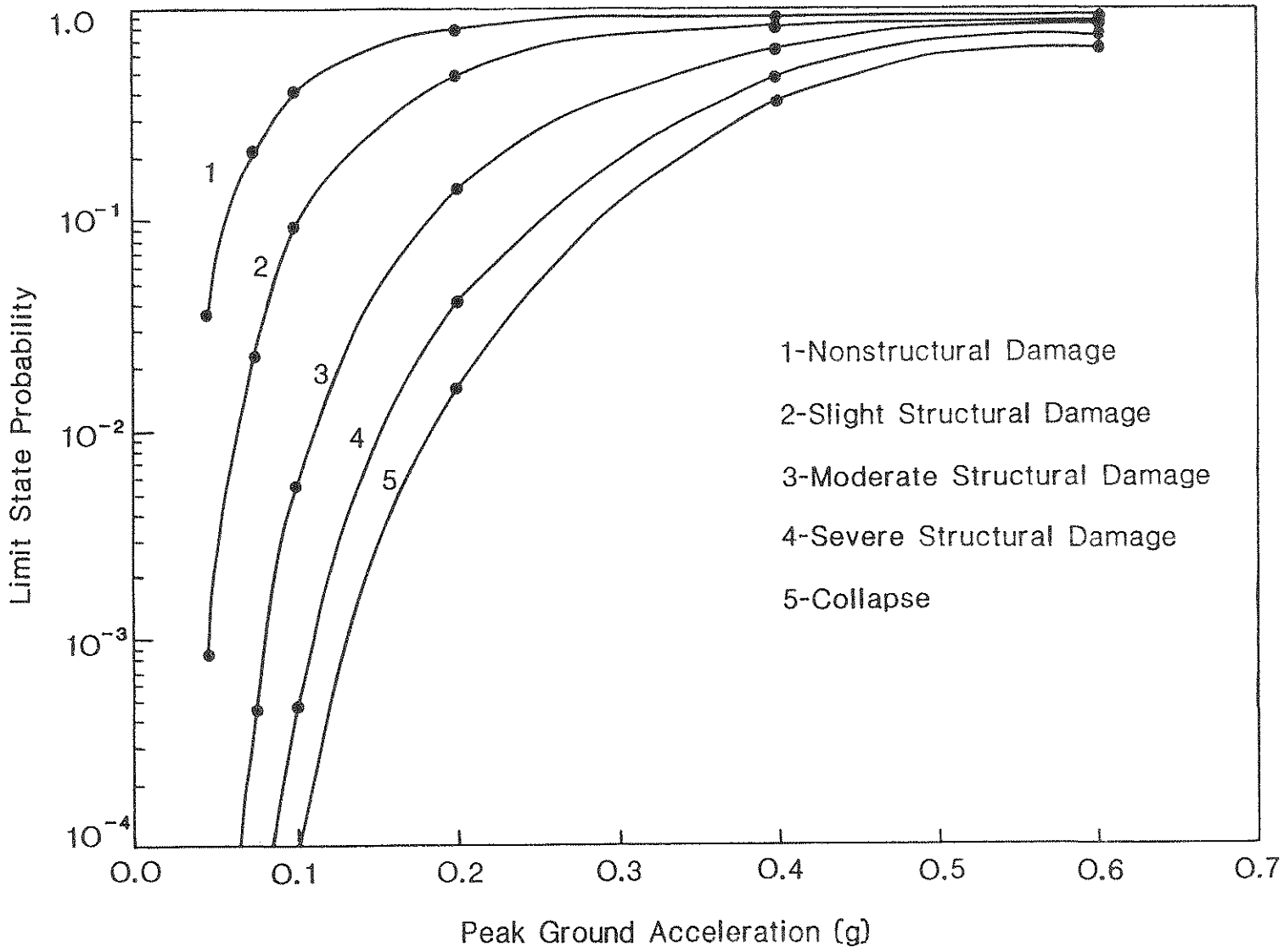

Fig. 3-8 Fragility Curves (Case I, Semi-Log Scale)

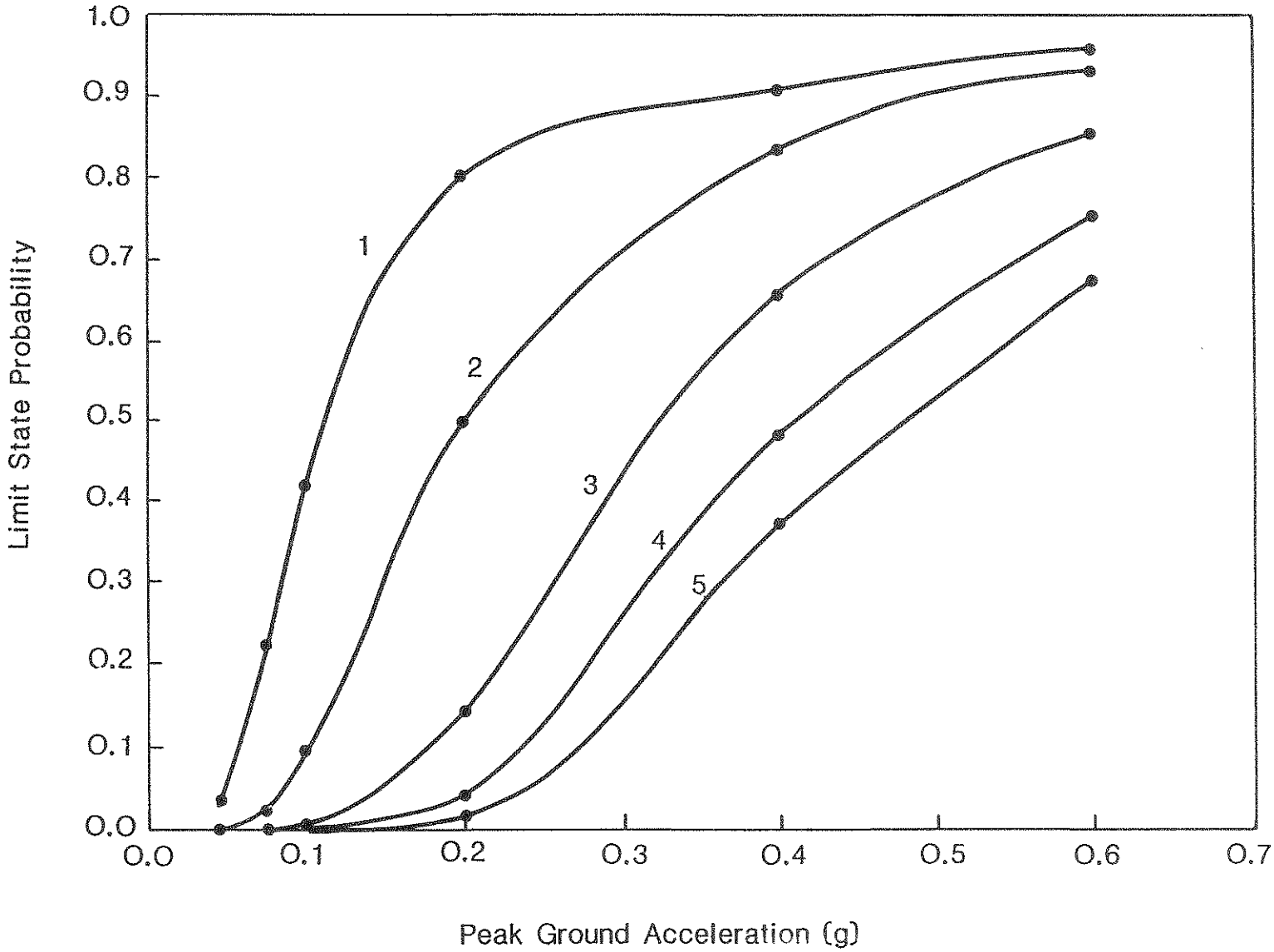

Fig. 3-9 Fragility Curves (Case I, Arithmetic Scale)

Table 3-VIII Fragility Data (Case II)

Limit State	Peak Ground Acceleration (g)					
	0.045	0.075	0.1	0.2	0.4	0.6
Nonstructural Damage	3.71 E-2	0.21	0.39	0.84	0.99	1.0
Slight Structural Damage	1.32 E-3	2.49 E-2	8.85 E-2	0.47	0.91	0.99
Moderate Structural Damage	1.18 E-5	9.38 E-4	7.79 E-3	0.13	0.65	0.91
Severe Structural Damage	3.86 E-7	7.84 E-5	1.17 E-3	4.04 E-2	0.44	0.78
Collapse	4.76 E-8	1.67 E-5	3.52 E-4	1.85 E-2	0.32	0.67

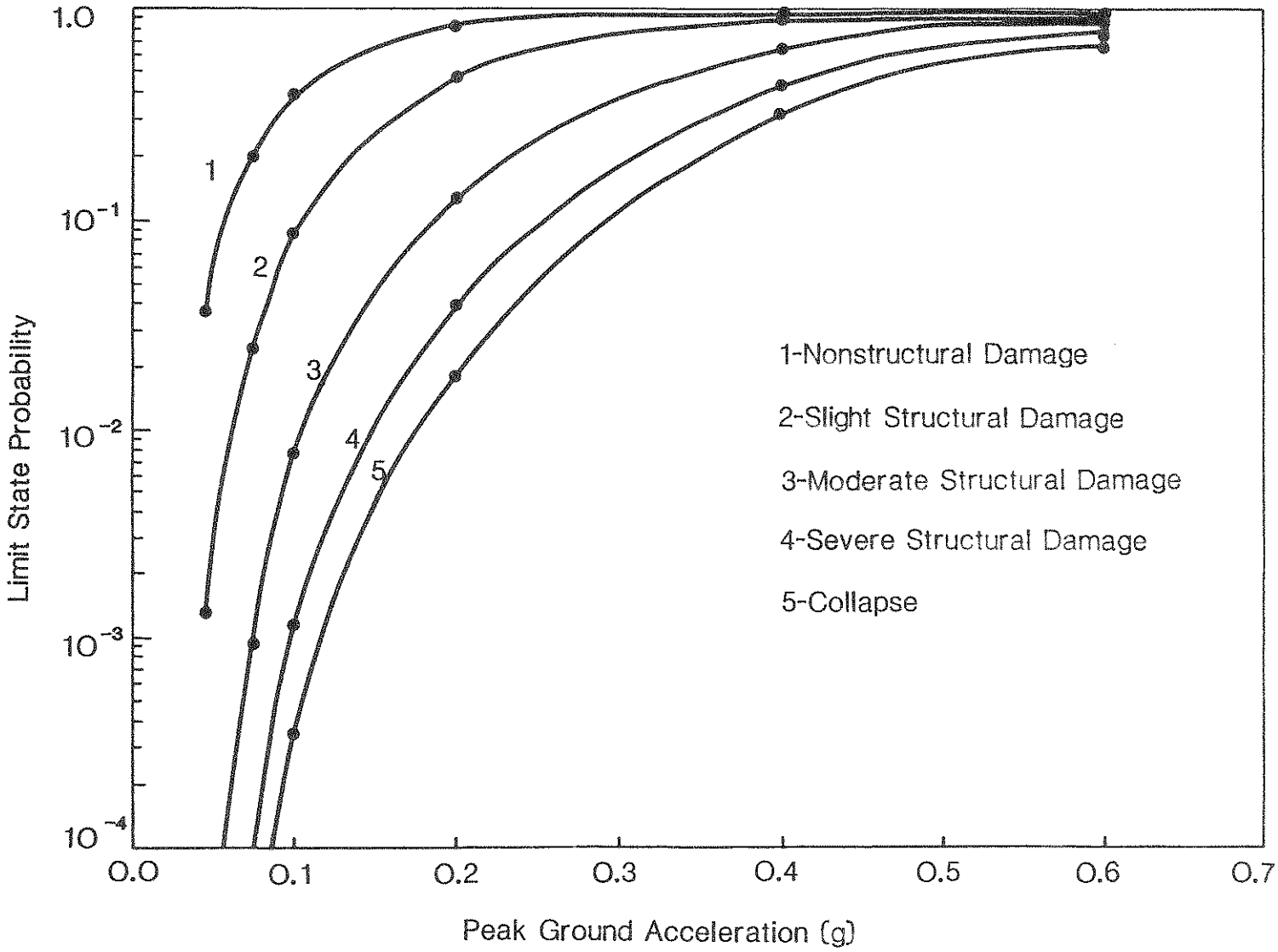

Fig. 3-10 Fragility Curves (Case Ⅱ)

are shown in Tables 3-VII and 3-VIII, respectively. From these two tables, it is clearly indicated that the limit state probabilities are compatible with each other.

(5) In order to ensure the safety of structures, the conservatism is built in at each step of the design process. As a result, the actual structural capacity is usually larger than the design capacity, however, the actual capacity is unknown to the engineers. For the practical purpose, engineers are interested in the minimum actual capacity. It is recommended that the minimum actual capacity with respect to a specified limit state is set as the PGA value with the limit state probability of one percent. This minimum capacity is equivalent to the HCLPF value used in the margin studies for nuclear structures [2]. For the moderate damage limit state, the minimum capacity of the shear wall structure considered in this study is estimated as $0.113g$. This means that if an $0.1g$ earthquake occurs, the engineers are sure that the structure will not sustain any moderate damage. Furthermore, the minimum safety factor can be defined as the ratio of the minimum actual capacity in terms of PGA level to the design peak ground acceleration. Since the structure is designed for about $0.045g$ [21], the minimum safety factor for this shear wall structure is about 2.5 against moderate damage due to $0.1g$ earthquakes.

SECTION 4
CONCLUSIONS

This report presents a fragility analysis method for the generation of seismic fragility curves for structures, in particular, shear wall structures. The important features of the proposed method are as follows

(1) Uncertainties including randomness and modeling uncertainty in earthquake ground motion and structure are quantified by evaluating uncertainties in pertinent parameters which define the analytical model of the earthquake load-structure system. The advantage of this approach is that the assessment of uncertainty can be easily verified independently. As a result, the fragility data are more reliable.

(2) The nonlinear structural response is explicitly included in the fragility estimation by using the Latin hypercube sampling technique and appropriate hysteretic model. The utilization of the Latin hypercube sampling technique makes the probabilistic nonlinear time history analysis economic and feasible.

The fragility curves generated by the proposed method can be utilized in the seismic risk study to determine potential earthquake-induced loss of life and damage of properties, then the economic and societal risk can be estimated. In addition, the fragility data can be used by the authority to develop emergency response plan.

SECTION 5
REFERENCES

1. Applied Technology Council, "Earthquake Damage Evaluation Data for California," ATC-13, Redwood City, California, 1985.
2. Hwang, H., "Seismic Probabilistic Risk Assessment and Seismic Margins Studies for Nuclear Power Plants," Technical Report NCEER-87-0011, National Center for Earthquake Engineering Research, SUNY, Buffalo, New York, June 1987.
3. Smith, P.D., et al., "Seismic Safety Margins Research Program, Phase I Final Report," NUREG/CR-2015, Volumes 1-10, U.S. Nuclear Regulatory Commission, Washington, D.C., September 1982.
4. Kennedy, R.P. and Ravindra, M.K., "Seismic Fragilities for Nuclear Power Plant Risk Studies," Nuclear Engineering and Design, Vol. 79, May 1984, pp. 47-68.
5. Hwang, H., Reich, M., and Shinozuka, M., "Structural Reliability Analysis and Seismic Risk Assessment," in Seismic Events Probabilistic Risk Assessments, PVP-Vol. 79, ASME, 1984.
6. Federal Emergency Management Agency, "An Assessment of Damage and Casualties for Six Cities in the Central United States Resulting from Earthquakes in the New Madrid Seismic Zone," Report for Central United States Earthquake Preparedness Project, Washington, D.C., October 1985.
7. Kircher, C.A. and McCann, Jr., M.W., "Development Seismic Fragility Curves for Sixteen Types of Structures Common to Cities of the Mississippi Valley Region," Report prepared for Allen and Hoshall, Inc. Memphis, Tennessee, November 1984.
8. Nuclear Regulatory Commission, "PRA Procedures Guide," NUREG/CR-2300, Vols. 1 and 2, Washington, D.C., January 1983.
9. Hwang, H., Jaw, J.-W., and Shau, H.-J., "Seismic Performance Assessment of Code-Designed Structures," Technical Report NCEER-88-0007, National Center for Earthquake Engineering Research, SUNY, Buffalo, New York, 1988.
10. Shinozuka, M., "Digital Simulation of Random Process in Engineering Mechanics with the Aid of FFT Technique," Stochastic Problems in Mechanics, S.T. Ariaratnam and H.E.E. Liepholz, eds., University of Waterloo press, Waterloo, Ontario, Canada, 1974.
11. Tajimi, H., "A Statistical Method of Determining the Maximum Response of a Building Structure During an Earthquake," Proceedings of the 2nd World Conference on Earthquake Engineering, Tokyo, Vol. II, July 1960, pp. 781-798.

12. Shinozuka, M., Hwang, H., and Reich, M., "Reliability Assessment of Reinforced Concrete Containment Structures," Nuclear Engineering and Design, Vol. 80, 1984, pp. 247-267.

13. Lai, P. S.-S., "Statistical Characterization of Strong Ground Motions Using Power Spectral Density Functions," Bulletin of the Seismological Society of America, Vol. 72, No. 1, Feb. 1982, pp. 259-274.

14. Sues, R.H., Wen, Y.K., and Ang, A. H.-S., "Stochastic Evaluation of Seismic Structural Performance," Journal of Structural Engineering, ASCE, Vol. 111, No. 6, June 1985, pp. 1204-1218.

15. Ellingwood, B.R. and Batts, M.E., "Characterization of Earthquake Forces for Probability-based Design of Nuclear Structures," NUREG/CR-2945, U.S. Nuclear Regulatory Commission, Washington, D.C., September 1982.

16. Iman, R.L. and Conover, W.J., " Small Sample Sensitivity Analysis Techniques for Computer Models, With an Application to Risk Assessment," Communications in Statistics, Vol. A9, No. 17, 1980, pp. 1749-1842.

17. Hwang, H., et al., "Probability Based Load Combination Criteria for Design of Concrete Containment Structures," NUREG/CR-3876, U.S. Nuclear Regulatory Commission, March 1985.

18. Chung, Y.S., Meyer, C., and Shinozuka, M., "Seismic Damage Assessment of Reinforced Concrete Members," Technical Report NCEER-87-0022, National Center for Earthquake Engineering Research, SUNY, Buffalo, New York, October 1987.

19. Ellingwood, B. and Hwang, H., "Probabilistic Descriptions of Resistance of Safety-related Structures in Nuclear Power Plants," Nuclear Engineering and Design, Vol. 88, 1985, pp. 169-178.

20. Ang, A. H.-S., and Tang, W. H., *Probability Concepts In Engineering Planning And Design*, Vol. II, John Wiley and Sons, Inc., New York, 1984.

21. Hwang, H., Ushiba, H., and Shinozuka, M., "Reliability Analysis of Code-Designed Structure Under Natural Hazards," NCEER Technical Report (in print).

22. American National Standard Institute, *Minimum Design Loads for Buildings and other Structures*, ANSI A58.1-1982, New York, 1982.

23. American Concrete Institute, *Building Code Requirements for Reinforced Concrete*, ACI 318-83, Detroit, Michigan.

24. Newmark, N.M., "Inelastic Design of Nuclear Reactor Structures and its Implications on Design of Critical Equipment," Transaction of the 4th International SMiRT

Conference, San Francisco, August 1977, Vol. K(a), paper K4/1.

25. Bennett, J.G., Dove, R.C., Dunwoody, W.E., and Farrar, C., "Latest Results from the Seismic Category I Structures Program," Nuclear Engineering and Design, Vol. 94, 1986, pp. 25-29.
26. Morgan, B., Hiraishi, H., and Corley, W.G., "Medium Scale Wall Assemblies: Comparison of Analysis and Test Results," ACI Special publication SP-84, Earthquake Effects on Reinforced Concrete Structure for U.S.–Japan Research, Detroit, Michigan, 1984, pp. 241-269.
27. Oesterle, R.G., Aristizabal-Ochoa, J.D., Shiu, K.N., and Corley W.G., "Web Crushing of Reinforced Concrete Structural Walls," ACI Journal, Vol. 81, No. 3, May-June, 1984, pp. 231-241.
28. Tohma, J. and Hwang, H., "Hysteretic Model for Reinforced Concrete Containment," Transaction of the 9th International SMiRT Conference, Lausanne, Switzerland, August 1987, Vol. H, pp. 251-256.
29. Hwang, H., Low, Y.K., Jaw, J.-W., and Chang, T.-S., "Soil Effects on Strong Earthquake Acceleration in Memphis Area," CERI Technical Report, Memphis State University, February 1988.
30. Aktan, A.E. and Bertero, V.V., "RC Structural Walls: Seismic Design For Shear," Journal of Structural Engineering, ASCE, Vol. 111, No. 8, August 1985, pp. 1775-1791.

NATIONAL CENTER FOR EARTHQUAKE ENGINEERING RESEARCH
LIST OF PUBLISHED TECHNICAL REPORTS

The National Center for Earthquake Engineering Research (NCEER) publishes technical reports on a variety of subjects related to earthquake engineering written by authors funded through NCEER. These reports are available from both NCEER's Publications Department and the National Technical Information Service (NTIS). Requests for reports should be directed to the Publications Department, National Center for Earthquake Engineering Research, State University of New York at Buffalo, Red Jacket Quadrangle, Buffalo, New York 14261. Reports can also be requested through NTIS, 5285 Port Royal Road, Springfield, Virginia 22161. NTIS accession numbers are shown in parenthesis, if available.

NCEER-87-0001 "First-Year Program in Research, Education and Technology Transfer," 3/5/87, (PB88-134275/AS).

NCEER-87-0002 "Experimental Evaluation of Instantaneous Optimal Algorithms for Structural Control," by R.C. Lin, T.T. Soong and A.M. Reinhorn, 4/20/87, (PB88-134341/AS).

NCEER-87-0003 "Experimentation Using the Earthquake Simulation Facilities at University at Buffalo," by A.M. Reinhorn and R.L. Ketter, to be published.

NCEER-87-0004 "The System Characteristics and Performance of a Shaking Table," by J.S. Hwang, K.C. Chang and G.C. Lee, 6/1/87, (PB88-134259/AS).

NCEER-87-0005 "A Finite Element Formulation for Nonlinear Viscoplastic Material Using a Q Model," by O. Gyebi and G. Dasgupta, 11/2/87, (PB88-213764/AS).

NCEER-87-0006 "Symbolic Manipulation Program (SMP) - Algebraic Codes for Two and Three Dimensional Finite Element Formulations," by X. Lee and G. Dasgupta, 11/9/87.

NCEER-87-0007 "Instantaneous Optimal Control Laws for Tall Buildings Under Seismic Excitations," by J.N. Yang, A. Akbarpour and P. Ghaemmaghami, 6/10/87, (PB88-134333/AS).

NCEER-87-0008 "IDARC: Inelastic Damage Analysis of Reinforced Concrete-Frame Shear-Wall Structures," by Y.J. Park, A.M. Reinhorn and S.K. Kunnath, 7/20/87, (PB88-134325/AS).

NCEER-87-0009 "Liquefaction Potential for New York State: A Preliminary Report on Sites in Manhattan and Buffalo," by M. Budhu, V. Vijayakumar, R.F. Giese and L. Baumgras, 8/31/87, (PB88-163704/AS).

NCEER-87-0010 "Vertical and Torsional Vibration of Foundations in Inhomogeneous Media," by A.S. Veletsos and K.W. Dotson, 6/1/87, (PB88-134291/AS).

NCEER-87-0011 "Seismic Probabilistic Risk Assessment and Seismic Margin Studies for Nuclear Power Plants," by Howard H.M. Hwang, 6/15/87, (PB88-134267/AS).

NCEER-87-0012 "Parametric Studies of Frequency Response of Secondary Systems Under Ground-Acceleration Excitations," by Y. Yong and Y.K. Lin, 6/10/87, (PB88-134309/AS).

NCEER-87-0013 "Frequency Response of Secondary Systems Under Seismic Excitations," by J.A. HoLung, J. Cai and Y.K. Lin, 7/31/87, (PB88-134317/AS).

NCEER-87-0014 "Modelling Earthquake Ground Motions in Seismically Active Regions Using Parametric Time Series Methods," G.W. Ellis and A.S. Cakmak, 8/25/87, (PB88-134283/AS).

NCEER-87-0015 "Detection and Assessment of Seismic Structural Damage," by E. DiPasquale and A.S. Cakmak, 8/25/87, (PB88-163712/AS).

NCEER-87-0016 "Pipeline Experiment at Parkfield, California," by J. Isenberg and E. Richardson, 9/15/87, (PB88-163720/AS).

NCEER-87-0017 "Digital Simulations of Seismic Ground Motion," by M. Shinozuka, G. Deodatis and T. Harada, 8/31/87, (PB88-155197/AS).

NCEER-87-0018 "Practical Considerations for Structural Control: System Uncertainty, System Time Delay and Truncation of Small Forces," J. Yang and A. Akbarpour, 8/10/87, (PB88-163738/AS).

NCEER-87-0019 "Modal Analysis of Nonclassically Damped Structural Systems Using Canonical Transformation," by J.N. Yang, S. Sarkani and F.X. Long, 9/27/87, (PB88-187851/AS).

NCEER-87-0020 "A Nonstationary Solution in Random Vibration Theory," by J.R. Red-Horse and P.D. Spanos, 11/3/87, (PB88-163746/AS).

NCEER-87-0021 "Horizontal Impedances for Radially Inhomogeneous Viscoelastic Soil Layers," by A.S. Veletsos and K.W. Dotson, 10/15/87, (PB88-150859/AS).

NCEER-87-0022 "Seismic Damage Assessment of Reinforced Concrete Members," by Y.S. Chung, C. Meyer and M. Shinozuka, 10/9/87, (PB88-150867/AS).

NCEER-87-0023 "Active Structural Control in Civil Engineering," by T.T. Soong, 11/11/87, (PB88-187778/AS).

NCEER-87-0024 "Vertical and Torsional Impedances for Radially Inhomogeneous Viscoelastic Soil Layers," by K.W. Dotson and A.S. Veletsos, 12/87, (PB88-187786/AS).

NCEER-87-0025 "Proceedings from the Symposium on Seismic Hazards, Ground Motions, Soil-Liquefaction and Engineering Practice in Eastern North America, October 20-22, 1987, edited by K.H. Jacob, 12/87, (PB88-188115/AS).

NCEER-87-0026 "Report on the Whittier-Narrows, California, Earthquake of October 1, 1987," by J. Pantelic and A. Reinhorn, 11/87, (PB88-187752/AS).

NCEER-87-0027 "Design of a Modular Program for Transient Nonlinear Analysis of Large 3-D Building Structures," by S. Srivastav and J.F. Abel, 12/30/87, (PB88-187950/AS).

NCEER-87-0028 "Second-Year Program in Research, Education and Technology Transfer," 3/8/88.

NCEER-88-0001 "Workshop on Seismic Computer Analysis and Design With Interactive Graphics," by J.F. Abel and C.H. Conley, 1/18/88, (PB88-187760/AS).

NCEER-88-0002 "Optimal Control of Nonlinear Structures," J.N. Yang, F.X. Long and D. Wong, 1/22/88, (PB88-213772/AS).

NCEER-88-0003 "Substructuring Techniques in the Time Domain for Primary-Secondary Structural Systems," by G. D. Manolis and G. Juhn, 2/10/88, (PB88-213780/AS).

NCEER-88-0004 "Iterative Seismic Analysis of Primary-Secondary Systems," by A. Singhal, L.D. Lutes and P. Spanos, 2/23/88, (PB88-213798/AS).

NCEER-88-0005 "Stochastic Finite Element Expansion for Random Media," P. D. Spanos and R. Ghanem, 3/14/88, (PB88-213806/AS).

NCEER-88-0006 "Combining Structural Optimization and Structural Control," F. Y. Cheng and C. P. Pantelides, 1/10/88, (PB88-213814/AS).

NCEER-88-0007 "Seismic Performance Assessment of Code-Designed Structures," H.H-M. Hwang, J. Jaw and H. Shau, 3/20/88.

NCEER-88-0008 "Reliability Analysis of Code-Designed Structures Under Natural Hazards," H.H-M. Hwang, H. Ushiba and M. Shinozuka, 2/29/88.

NCEER-88-0009 "Seismic Fragility Analysis of Shear Wall Structures," J-W Jaw and H.H-M. Hwang, 4/30/88.

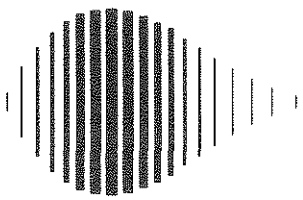

National Center for Earthquake Engineering Research
State University of New York at Buffalo